



People's Democratic Republic of Algeria
Ministry of Higher Education and Scientific Research
Kasdi Merbah University Ouargla



Faculty of Hydrocarbons, Renewable Energies and Earth and Universe Sciences
Renewable Energies Department

Memory Presented for obtaining the diploma of MASTER

Field: electrotechnics

Specialty: Renewable Energies in electrotechnics

Presented by:

Bedaa Safieddine

Terriche Abdelmadjid

Entitled:

***Enhancement study of the efficiency of photovoltaic panels
through the utilization of geothermal cooling system***

Discussed publicly on: 6/6/2024.

Before the jury composed of:

Djamel	belatrache	Dr.	Chairman	Kasdi Merbah University Ouargla
Djamel	Benmenine	Dr.	Supervisor	Kasdi Merbah University Ouargla
Abdessamia	Hadjadj	Dr.	Examiners	Kasdi Merbah University Ouargla

Academic year: 2023/2024

Thanks

First of all, we would like to thank our Allah, our creator for giving us the strength to accomplish this work.

We would like to express our sincere thanks to all the teachers who helped us throughout our university studies, in particular our supervisor Dr. Benmenine Djamel for his advice and the help he gave us.

We would also like to express our gratitude to:

Mr. Benali Oussama for guidance and advice.

Mr. Abdessamia Hadjadj My thanks also go to all those who contributed, directly or indirectly, to the accomplishment of this work, and in particular:

Mr. Djamel belatrache Dr. at the University of Kasdi Merbah Ouargla, for having done me the honor

to chair my dissertation jury.

Our final thanks go to all those who contributed directly or indirectly to the completion of this work.

Dedication

Praise be to Allah and thanks to Allah Almighty for what He has honored me with and bestowed upon me, and prayers and peace be upon our master Muhammad, the most honorable of creation, the truthful and faithful, may Allah bless him and grant him peace.

Then I dedicate this work to:

My dear mother and honorable father for their support, help and patience, and my honorable wife, and my dear brothers and sisters, to all my teachers, each by name, to all my family, all my friends and loved ones in Allah, to all my colleagues, each by name, to every person who helped me. We ask Allah Almighty to grant us success in what He loves and pleases, and to grant us honesty in word and deed, and to make us among the heirs of the Garden of Bliss. Amen, for all.

Terriche Abdelmadjid

Dedication

Praise be to Allah and thanks to Allah Almighty for what He has honored me with and bestowed upon me, and prayers and peace be upon our master Muhammad, the most honorable of creation, the truthful and faithful, may Allah bless him and grant him peace.

Then I dedicate this work to:

My dear mother and honorable father for their support, assistance, support and patience with me, and my dear brothers and sisters, my support in this life, to all my honorable family, each by name, to all my teachers and everyone who taught me, to all my friends and loved ones in Allah, to all my colleagues, each by name, to each person. Help me, may you always be good, safe and reassured. I ask Allah Almighty to grant us success in word and deed and to make us among the heirs of the Garden of Bliss. Amen, for all.

Bedaa Safieddine

Contents

List of tables	i
List of figures.....	ii
Nomenclatures.....	iv
Abbreviations	iv
General introduction.....	1
Chapter I Generalities on photovoltaics	4
I.1. Introduction	5
I.2. Global electricity consumption.....	5
I.2.1. Renewable electricity	6
I.2.2. Global photovoltaic capacity	6
I.3. Photovoltaic cell and these characteristics	8
I.3.1. Photovoltaic cell.....	8
I.3.2. The principle of the work of the solar cell	9
I.3.3. Different types of photovoltaic solar cells	10
A. First generation solar cells.....	10
1. Monocrystalline cells.....	10
2. Poly-crystalline cells.....	11
B. Second generation solar cell Technology (Thin film solar cell technology)	12
1. Amorphous cells.....	12
2. Cadmium-telluride (CdTe).....	13
3. Gallium arsenic (copper-indium-di selenium (CIS) or copper-indium-gallium selenium (CIGS)).....	13
4. Copper Zinc Tin Sulphide (CZTS) Thin film solar cells	14
5. Compounds of group III-V.....	14
C. Third generation solar cell technology.....	15
1. CZTS solar cells including materials CZTSe and CZTSSe (Double Junction solar cells).....	15
2. Dye sensitized solar cells.....	17
3. Quantum Dot solar cells	17
4. Perovskite solar cells	17
5. Organic solar cells.....	18
I.3.4. The solar cell photovoltaic features	18
a. The short circuit current I_{sc}	19
b. The voltage of the circuit-ouverte V_{co}	19
c. The maximum power P_m	19
d. The form factor FF	20

e. The yield η	20
I.3.5. Assembly of solar cells (series, parallel, series-parallel).....	21
A. Serial association.....	21
B. Parallel association.....	21
C. Hybrid association (series/parallel).....	22
I.3.6. Photovoltaic applications	22
A. Autonomous systems (Isolated installations).....	23
B. Grid-connected systems.....	23
I.4. Conclusion.....	24
Chapter II Literature review of the PV cooling methods and systems by geothermal energy	25
II.1. Introduction	26
II.2. Environmental parameters affecting photovoltaic cells efficiency	26
II.2.1. Effect of radiation intensity	26
II.2.2. Temperature effect.....	26
II.2.3. Wind effect	27
II.2.4. Dust effect.....	27
II.2.5. Shading effect.....	27
II.2.6. Humidity effect.....	28
II.3. Literature review the PV cooling methods and systems by geothermal energy	28
II.4. Conclusion.....	34
Chapter III Methodology and Experimental study of the PV cooling system by geothermal energy	35
III.1. Introduction	36
III.2. Place of the conduct the experiments	36
III.3. Description of the experimental device.....	37
III.4. The different properties of the photovoltaic one used.....	40
III.5. Different measurement equipment for an experiment.....	42
III.6. Results and discussions	44
III.6.1. Cooling effect on thermal characteristics	47
III.6.2. Cooling effect on electrical characteristics.....	50
General conclusion.....	52
References.....	54
ملخص	57

List of tables

Table III-1: represents the specifications of polycrystalline PV modules used under STC standard test conditions.	40
Table III-2: represents details of the specifications of the various measuring devices used according to the technical data of the equipment manufacturers.	43
Table III-3: values Obtained of solar irradiation intensity (G) throughout the experimental test period.	45
Table III-4: values Obtained of ambient temperature (T_a) throughout the experimental test period.	45
Table III-5: values Obtained of wind velocity throughout the experimental test period.	46
Table III-6: values Obtained of temperature T_{c1} for the cooled and T_{r1} reference PV panels for the duration of the experiment	48
Table III-7: values Obtained of temperature T_2 for the cooled and reference PV panels for the duration of the experiment.	49
Table III-8: values Obtained of temperature T_3 for the cooled and reference PV panels for the duration of the experiment.	50
Table III-9: values Obtained of voltage for the cooled and reference PV panels for the duration of the experiment.	51

List of figures

Figure I- 1: Structure standard of a solar cell	8
Figure I- 2: Diagram of the work of a solar cell	9
Figure I- 3: Various types of solar cells and current advancements.	10
Figure I- 4: Diagram of the monocrystalline PV panel and cell	11
Figure I- 5: Diagram of the poly-crystalline PV panel and cell.....	11
Figure I- 6: Schematic of the amorphous PV panel and cell.	12
Figure I- 7: diagram of the structure and Cadmium Telluride (CdTe) PV panel.	13
Figure I- 8: CIGS structure and PV panel diagram	13
Figure I- 9: Schematic of one-dimensional substrate CZTS solar cells.....	14
Figure I- 10: Compounds of group III-V cell structure diagram.....	15
Figure I- 11: Schematic of Multi junction solar cell.....	16
Figure I- 12: Crystal structure of organometal perovskite.	18
Figure I- 13: Diagram of the structure of organic solar cells.....	18
Figure I- 14: Maximum power point of an elementary cell.	19
Figure I- 15: Features derived by sequentially grouping rows of the same cells.....	21
Figure I- 16: Features derived by grouping rows on branches of the same cells.....	21
Figure I- 17: Features derived by grouping rows on a sequence and branching, from the same cells.	22
Figure I- 18: Schematic of a stand-alone PV system.....	23
Figure I- 19: Schematic diagram of a grid connected PV system.	24
Figure II- 1: Characteristics of a solar P·V.: Effect of solar irradiance.....	26
Figure II- 2: Characteristics of a solar P·V.: Effect of solar temperature.....	27
Figure II- 3: Schematic design of ground coupled-central panel cooling system (GC-CPCS)..	29
Figure II- 4: Schematic of PV air cooling with buried heat exchanger	29
Figure II- 5: A schematic diagram of the experimental setup	31
Figure II- 6: the schematic diagram of the system.	32
Figure II- 7: Schematic connections of the designed PV panel with cooling system.....	33
Figure II- 8: Schematic diagram of a simplified PV-GHEs system.	34
Figure III- 1: Average annual temperature for Algeria, and Ouargla State.....	37
Figure III- 2: A general display of the system used for the cooling of photovoltaic panels.	38
Figure III- 3: Schematic diagram of the experimental process of the cooling system.	39
Figure III- 4: A variable flow extractor (50-Watt portable fan).....	39
Figure III- 5: The cover used in the experimental study.....	41
Figure III- 6: The cover and connected photovoltaic panel used in the experimental study.	41
Figure III- 7: Front view of the experimental setup.....	42
Figure III- 8: Distribution method for K-type thermocouples.....	43
Figure III- 9: Evolution of solar radiation intensity (G) throughout the experimental test period.	45
Figure III- 10: Evolution of ambient temperature (Ta) throughout the experimental test period.	46
Figure III- 11: Evolution of wind velocity throughout the experimental test period.	47
Figure III- 12: Evolution of temperature Tc1 for the cooled and Tr1 reference PV panels throughout the experimental test period.....	48
Figure III- 13: Evolution of temperature Tc2 for the cooled and Tr2 reference PV panels throughout the experimental test period.....	49

Figure III- 14: Evolution of temperature T_{c3} for the cooled and T_{r3} reference PV panels throughout the experimental test period.....	50
Figure III- 15: Evolution of voltage for the cooled and reference PV panels throughout the experimental test period.	51

Nomenclatures

G	Solar radiation (W/m²)
T	Temperature (°C)
t	Time (s)
V	PV modules' voltage (V)
I	PV modules' current (A)
P_m	Maximum output power (W)
I_{sc}	Short-circuit current
V_{oc}	Open-circuit Voltage
T_a	Ambient temperature (°C)
T_c	Temperature of cooled PV module (°C)
T_r	Temperature of reference PV module (°C)
FF	Fill Factor
I_m	Maximum current
V_m	Maximum voltage
W	Watt
TWh	Tera watt courier
GW	Giga watt

Abbreviations

PV	Photovoltaic
IEA	International Energy Agency
AI	artificial intelligence
CdTe	Cadmium-Telluride
CIGS	Cooper-Indium-Gallium Selenium
CZTS	Copper Zinc Tin Sulphide
GaAS	Gallium Arsenide
InGaP	Indium Gallium Phosphide
NREL	National Renewable Energy Laboratory
DSSC	Dye Sensitized Solar Cell
QDs	Quantum Dot Solar Cell

BIPV	Building-integrated photovoltaic
CFD	Dynamic fluid computational
CPV	Concentrated photovoltaic
TEG	Thermoelectric generator
PCM	Phase Change Materials
PV/T	Photovoltaic/Thermal
PVC	Poly Vinyl Chloride
STC	Standard Test Conditions

General introduction

In this world, people live in an energy-intensive and consumption-based environment. This has led to a rapid collapse of fossil fuels, which are the main basis for electricity production. Therefore, it is very necessary to find sustainable energy sources to reduce our dependence on fossil fuels [1]. Renewable energies are the only and main alternative to traditional fossil energies.

Renewable energy is a kind of energy generated by natural resources and constantly renewed. It is different from non-renewable energy that will be exhausted after being consumed in large quantities. It has many advantages such as protecting the environment and avoiding the generation of greenhouse gases. It is considered environmentally friendly, its natural resources are constantly renewable, and it is economical. These include solar energy, wind energy, hydro energy, geothermal energy, etc.

Renewable energy faces many challenges, including dependence on weather and climate conditions and the need to develop technologies to make them more efficient and provide more energy.

Solar energy is the commonly used non-conventional energy available all over the world. Solar radiation is the source of all types of renewable energy. It can be converted directly or indirectly into electrical energy either through photovoltaic cells or thermal collectors, respectively [1].

Photovoltaics (PV) is one of the most established solar energy conversion technologies, converting solar energy directly into electricity with unlimited potential, quieter operation and low maintenance costs. A photovoltaic cell is essentially a junction diode. Photovoltaic solar cells are one form. A photovoltaic cell is defined as a device whose electrical properties (such as voltage, current, or resistance) change when exposed to light. Individual solar cells can be combined into modules, often called solar panels. Single-junction silicon solar cells can produce a maximum open circuit voltage of about 0.5 to 0.6 volts. That's not a lot on its own, but keep in mind that these solar cells are very small and when combined into one large solar panel can produce a significant amount of renewable energy [2].

The efficiency of a photovoltaic cell is affected by many factors, most notably the rise in ambient temperature, which is what characterizes the state of Ouargla in southern

Algeria, which is known for its high temperatures in summer. This constitutes an obstacle to the performance of photovoltaic cells, so we resort to photovoltaic cooling methods as a solution to the problem of the high temperature of the panels PV.

Cooling technologies can be implemented using alternative energies. Therefore, geothermal energy can be used for cooling. It is one of the types of renewable energy that refers to energy stored in the ground. So much so that primary energy is consumed mainly in the form of heat and comes from the Earth. By exploiting the Earth's thermal inertia using an air-ground exchanger. An air-ground exchanger is a system that uses the Earth's interior as an energy source and air as a heat exchange medium. The air sucked in from the outside passes through a tube buried underground at a well-defined depth, and along the tube it recovers the thermal energy of the earth by forced convection to cool or heat itself depending on whether it is winter or Summer [3].

In this work we will study the effect of a geothermal cooling system on the thermal and electrical properties of photovoltaic panels. The memorandum is organized as follows:

We start with a general introduction. Then we go to the first chapter, in which we present global electricity consumption, including the possibilities of renewable energies in the world and the contribution of photovoltaic energy in the world. We also present generalities about photovoltaic cells, such as their concept, principle of operation, types of photovoltaic cells, and their electrical properties...etc.

In the second chapter, we review the most important environmental factors affecting photovoltaic cells, such as the effect of solar radiation intensity, the effect of temperature, etc. This chapter also presents photovoltaic cooling technologies, mentioning previous studies for each photovoltaic cooling technology.

In the third chapter, the proposed experimental study to study the effect of a geothermal cooling system on the thermal and electrical properties of photovoltaic panels is presented and described, and the results obtained are discussed.

We conclude the work with a general conclusion.

Chapter I Generalities on photovoltaics

I.1. Introduction

Excessive consumption of traditional fossil energies resulted in an energy crisis and an increase in environmental concerns, and dense emissions from harmful greenhouse gases that cause global warming, threatening the security of people and the future of the world [4]. Demands for renewable and clean energies have increased to reduce dependence on traditional fossil energies and reduce associated environmental concerns. Solar energy is the best source of renewable energy due to its cleanliness, accessibility, sustainability and unlimited potential [5].

Photovoltaic conversion is direct conversion of electromagnetic energy (radiation) into direct current electrical energy. The main ingredient in this conversion is solar photovoltaic cell [6].

In this chapter, generalities of solar photovoltaic are shown.

I.2. Global electricity consumption

Global electricity demand grew moderately in 2023, but growth will accelerate through 2026. Electricity consumption in developed countries restrained the growth of global electricity demand in 2023: global electricity demand growth in 2023 was 2.2%, lower than the 2.4% growth observed in 2022. While China, India and numerous countries in Southeast Asia experienced robust growth in electricity demand in 2023, advanced economies posted substantial declines due to a lackluster macroeconomic environment and high inflation, which reduced manufacturing and industrial output [7].

Global electricity demand is expected to increase at a faster pace over the next three years, growing at an average annual rate of 3.4% through 2026. This growth will be driven by improved economic prospects, which will contribute to accelerated electricity demand growth in both developed and emerging economies. Particularly in developed countries and China, electricity demand will be supported by the increasing electrification of the residential and transportation sectors and a marked expansion of the data center sector. The share of electricity in final energy consumption is estimated to reach 20% by 2023, up from 18% in 2015. While this is progress, electrification needs to accelerate rapidly to meet the world's decarbonization targets. In the **IEA's** Net Zero Emissions by 2050 Scenario, a

pathway aligned with limiting global warming to 1.5 °C, electricity's share in final energy consumption nears 30% in 2030 [7].

Power consumption by data centers, artificial intelligence (AI), and the cryptocurrency sector could double by 2026. Data centers are significant drivers of growth in electricity demand in many regions. Total data center power consumption, which consumed an estimated 460 terawatt-hours (TWh) worldwide in 2022, could reach over 1,000 TWh by 2026. This demand is roughly equivalent to Japan's electricity consumption. Updated regulations and technological improvements, including on efficiency, will be crucial to moderate the surge in energy consumption from data centers [7].

I.2.1. Renewable electricity

Global forecast summary 2023 marks a step change for renewable power growth over the next five years Renewable electricity capacity additions reached an estimated 507 GW in 2023, almost 50% The policies, which are higher than in 2022 and continue to be supported in more than 130 countries, have led to significant changes in global growth. This worldwide acceleration in 2023 was driven mainly by year-on-year expansion in the People's Republic of China's (hereafter "China") booming market for solar PV (+116%) and wind (+66%). Renewable energy will continue to grow over the next five years; As production costs increase, solar and wind energy will account for 96% of this. Are lower than for both fossil and non-fossil alternatives in most countries and policies continue to support them [7].

While renewables are currently the largest energy source for electricity generation in 57 countries, mostly thanks to hydropower, these countries represent just 14% of global power demand. By 2028, 68 countries will have renewables as their main power generation source but still only account for 17% of global demand [7].

I.2.2. Global photovoltaic capacity

The global PV cumulative capacity grew to 1.6 TW in 2023, up from 1.2 TW in 2022, with from 407.3 GW to 446 GW of new PV systems commissioned – and according to the plan for 150 GW of modules in global storage. After years of concerns about material and transportation costs, module prices have fallen across many supply chains and remain

competitive with PV despite the recent decline in electricity prices. Historical peaks in 2022 [8].

Market growth outside of China reached an honorable 30%, while China's own domestic growth was above 120% which explained the tremendous PV market development. While the number of countries with a schooling rate above 10 percent increased to 18 compared to last year, countries with smaller populations such as Spain, the Netherlands, Chile and Greece were the leaders, while countries with larger populations such as Germany and Japan were also in the top 10%. While grid congestion has become an issue, policy measures, technical solutions and storage are already providing workable solutions to enhance PV penetration [8].

Despite competition in many parts of the market in many countries, individual markets continue to feel supported by domestic electricity prices and policies. It is unclear whether local industrial projects launched in recent years will be successful, as the dramatic increase in China's industrial capacity has forced markets to outpace the rest of the world Demand and consequent record low module prices. Significant drops in PV module prices due to increased inventory, oversupply and competitive environment among manufacturers caused strain on local manufacturing [8].

PV played an important role in the reduction of the CO₂ emissions from electricity in 2023, with more than 75% of new renewable capacity installed in 2023, generating nearly 60% of generation from new renewable capacity [8].

Oversupply of PV modules in 2023 has shed a light on the difficulties to align production and demand in a very versatile environment: while production capacities increased significantly in China, Global demand is not only determined by restrictions in markets such as the USA, India, Korea and Australia. Outside of China, growth occurred in several countries. Uneven political support in some markets could also be attributed to the difficulties to develop local PV manufacturing facilities in an already inundated market [8].

I.3. Photovoltaic cell and these characteristics

I.3.1. Photovoltaic cell

The photovoltaic cell consists of two words: photo (which is a word from Greek roots meaning light) and voltaic (volt is a unit).

It is used to measure electrical energy, and thus photoelectricity means the direct conversion of solar rays into continuous electricity, which is a Composite part made of semi-conductor materials and is the smallest photovoltaic system [9].

The photovoltaic cell consists of several layers:

- The two main ones are sensitive to light (P) and (N).
- The N layer represents silicon, in which the number of electrons is predominant, in addition to a pentavalent element.
- The P layer represents the silicon material in which the number of gaps (holes) is predominant, in addition to a trivalent element.
- A layer of light-transparent glass is added to the front surface to increase the absorption of light photons and protect the cell.
- A metal layer, such as aluminum, for example, is added to the front and back surfaces to form the cell's electrodes.

The figure I-1 shows structure standard of a solar cell.

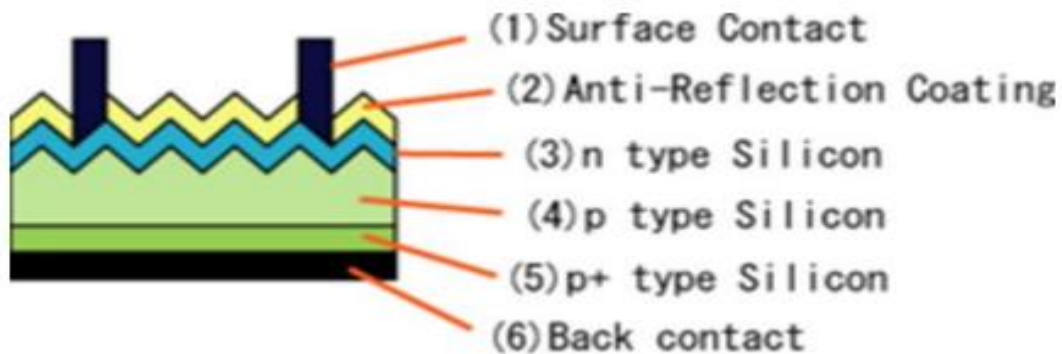


Figure I- 1: Structure standard of a solar cell [10].

I.3.2. The principle of the work of the solar cell

A photovoltaic cell is a device that performs conversion Solar energy into electrical energy. This transformation depends on three mechanisms explained as follows [6]:

- Absorption of photons (whose energy is greater than the gap) by the material constituting the device.
- Conversion of photon energy into electrical energy, which corresponds to the creation of electron/hole pairs in the semiconductor material.
- Collection of particles generated in the device.

The material constituting the photovoltaic cell must therefore have two energy levels and be sufficiently conductive to allow the flow of current, hence the interest in semiconductors for the photovoltaic industry. In order to collect the particles generated, an electric field allowing the electron/hole pairs created to be dissociated is necessary. For this we most often use a PN junction; other structures, such as hetero junctions and Schottky can also be used. The work of photovoltaic cells is illustrated in the **figure I-2** [6].

- Incident photons create carriers in the N and P zone and in the space charge zone [6].

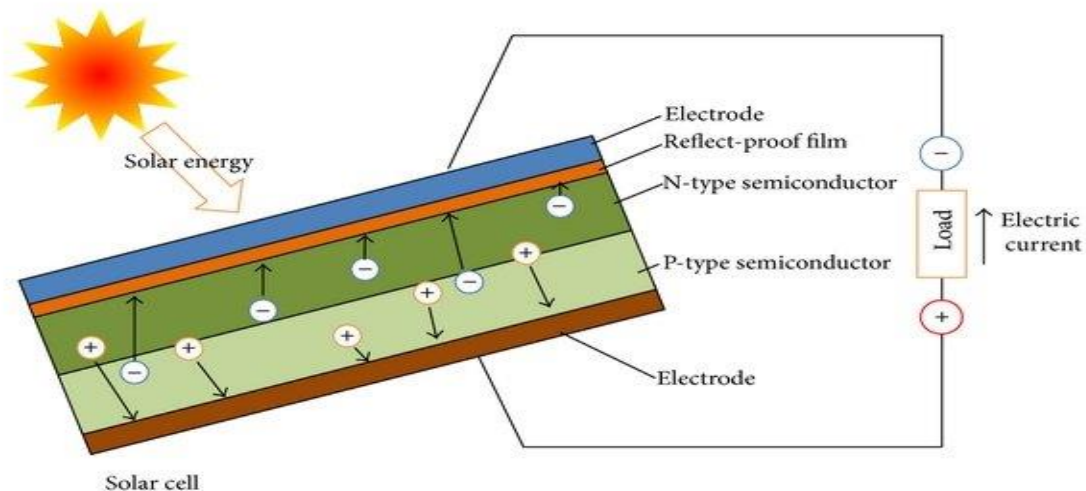


Figure I- 2: Diagram of the work of a solar cell [11].

I.3.3. Different types of photovoltaic solar cells

Figure I-3 shows different solar cell generation technologies [12].

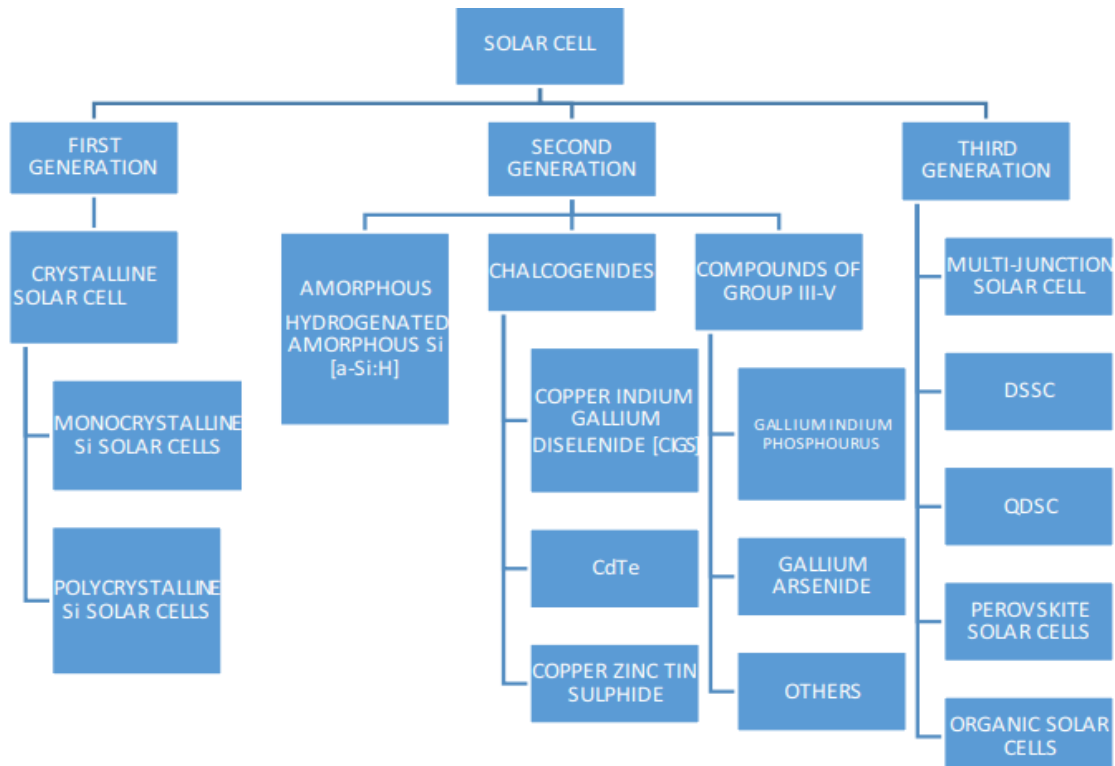


Figure I- 3: Various types of solar cells and current advancements [13].

A. First generation solar cells

Silicon is the basic material for solar cells. It is the second most abundant element in nature (it contains sand and quartz). There are three main categories of silicon solar cells:

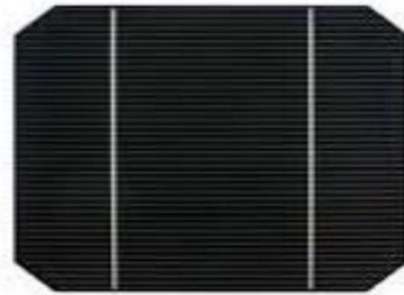
1. Monocrystalline cells

They are considered the first generation of solar cells and have an excellent efficiency rate [12]. (12-16% and up to 24% in the laboratory), but their production method is laborious and precise, and therefore very expensive. A large amount of energy is required to obtain pure crystal.

The figure I-4 shows diagram of the monocrystalline PV panel and cell.



Monocrystalline PV Panel



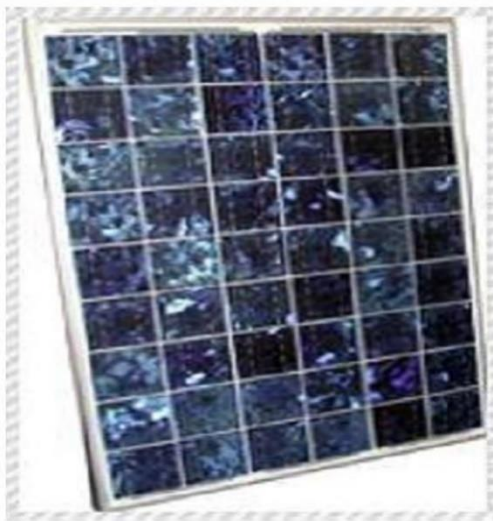
Monocrystalline Cell

Figure I- 4: Diagram of the monocrystalline PV panel and cell [14].

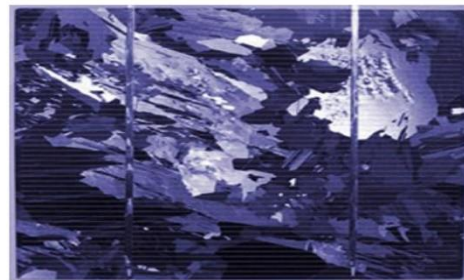
2. Poly-crystalline cells

They have a lower production cost than monocrystalline cells and a yield of 11-13% (about 18% in vitro) [12].

The figure I-5 shows diagram of the poly-crystalline PV panel and cell.



poly-crystalline PV panel



poly-crystalline cell

Figure I- 5: Diagram of the poly-crystalline PV panel and cell [14].

B. Second generation solar cell Technology (Thin film solar cell technology)

There are many techniques, including:

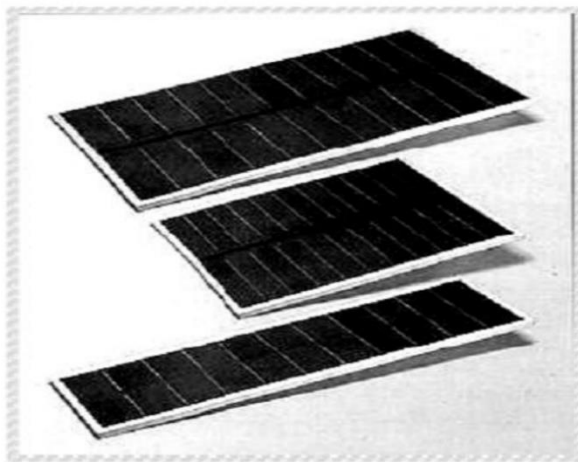
1. Amorphous cells

Their production cost is much lower, but also unfortunately, they have a lower yield of 8-10% (about 13% in vitro for non-lysed cells) [12].

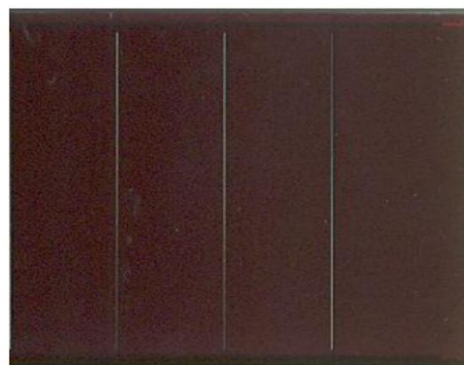
This technology allows the use of very thin layers of silicon of only 0.3 to 1.0 nm (500 nm for the other two types). We can therefore apply very thin layers of amorphous silicon to windows, metal or even flexible plastic using the vacuum evaporation process. It is an amorphous silicon often found in small consumer products such as calculators, watches, etc.

Amorphous panels require approximately twice the surface area (compared to crystalline panels) to produce the same amount of electricity, appear to degrade more quickly, but have the advantage of interacting better with diffuse and fluorescent light and performing better at high temperatures [12].

The figure I-6 shows schematic of the amorphous PV panel and cell.



amorphous PV Panel



amorphous Cell

Figure I- 6: Schematic of the amorphous PV panel and cell [14].

2. Cadmium-telluride (CdTe)

Yield 10.5% (15.8% in laboratory). High absorption, but let's not forget that cadmium is very toxic [15].

The figure I-7 shows diagram of the structure and Cadmium Telluride (CdTe) PV panel.

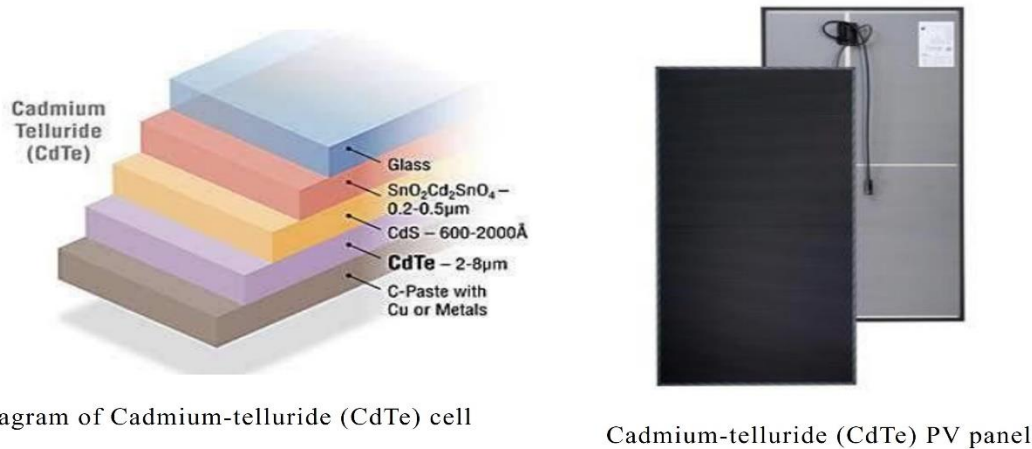


Diagram of Cadmium-telluride (CdTe) cell

Cadmium-telluride (CdTe) PV panel

Figure I- 7: diagram of the structure and Cadmium Telluride (CdTe) PV panel [16].

3. Gallium arsenic (copper-indium-di selenium (CIS) or copper-indium-gallium selenium (CIGS))

Their yield is equal to 11% (17.1% in the laboratory). 99% absorption, minimal degradation, but very delicate manufacturing [15].

The figure I-8 shows CIGS structure and PV panel diagram.

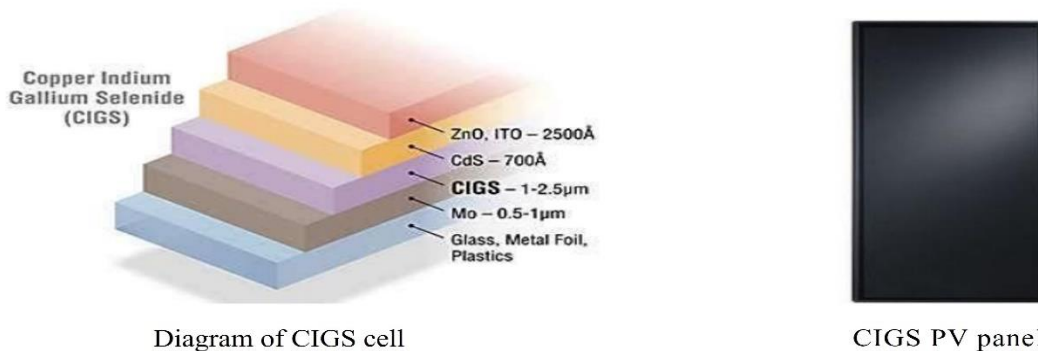


Diagram of CIGS cell

CIGS PV panel

Figure I- 8: CIGS structure and PV panel diagram [16].

4. Copper Zinc Tin Sulphide (CZTS) Thin film solar cells

Thin-film $\text{Cu}_2\text{ZnSnS}_4$ (CZTS) solar cells are a potential source of low-cost, high-efficiency solar cells. $\text{Cu}_2\text{ZnSnS}_4$ is a highly efficient thin-film absorber and a promising solar cell material. They found that the optical bandgap energy and absorption coefficient of CZTS. The optical bandgap energy and absorption coefficient of CZTS were about 1.5 eV and $1.0 \times 10^4 \text{ cm}^{-1}$, respectively. A high efficiency of 6.77% has been reported with an Al/ZnO: Al/CdS/CZTS/Mo/soda lime glass (SLG) substrate structure. Cadmium sulfide (CdS), zinc sulfide (ZnS), and zinc selenide (ZnSe) are used as buffer materials and zinc oxide (ZnO) as a window layer. (ZnO) is used as a window layer [17].

The figure I-9 shows Schematic of one-dimensional substrate CZTS solar cells.

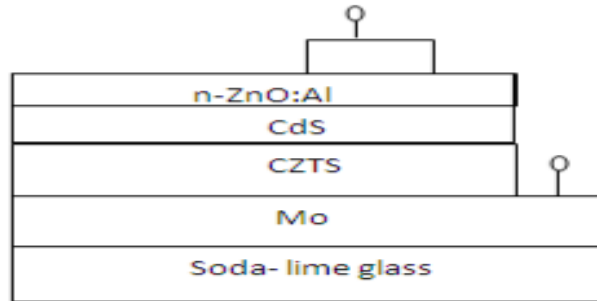


Figure I- 9: Schematic of one-dimensional substrate CZTS solar cells [17].

5. Compounds of group III-V

One of the main causes of solar cell efficiency loss is the energy loss of the solar cell due to a mismatch between the energy of the incident photons and the energy bandgap of the materials used. If the energy of the incident photon is less than the band gap energy of the material, the photon is not absorbed. If the energy of the incident photon is greater than the band gap energy of the material, the photon energy is lost. Therefore, by using multiple layers of photovoltaic materials with a wide range of bandgap energy values, a highly efficient III-V generation solar cell can be achieved to minimize photon energy loss and to absorb more photon energy from the broad solar spectrum incident on the solar cell. Thus, multi-junction solar cells consisting of multiple junctions are advantageous in achieving higher efficiencies: according to Shockley Queisser theory, if semiconductor materials with a bandgap energy of 1.34 eV

are used and the incident solar spectrum is considered to be AM1.5 [18], the theoretical maximum efficiency achieved with single-junction solar cell technology is GaAs is a typical III-V compound with a band gap close to about 1.42eV, making it a very suitable material for high efficiency thin film solar cells [19]. InGaP is a semiconductor composed of indium, gallium, and phosphorus with a lattice similar to that of GaAs [20]. Single-junction InGaP solar cells have been demonstrated to have a band gap energy of 1.81 eV and a solar conversion efficiency of 20.8% [21]. Since single-junction solar cells cannot absorb all photons from the spectrum of incoming sunlight, multi-junction solar cells with two or three junctions within the solar cell have been fabricated and demonstrated higher efficiencies.

The figure I-10 shows Compounds of group III-V cell structure diagram.

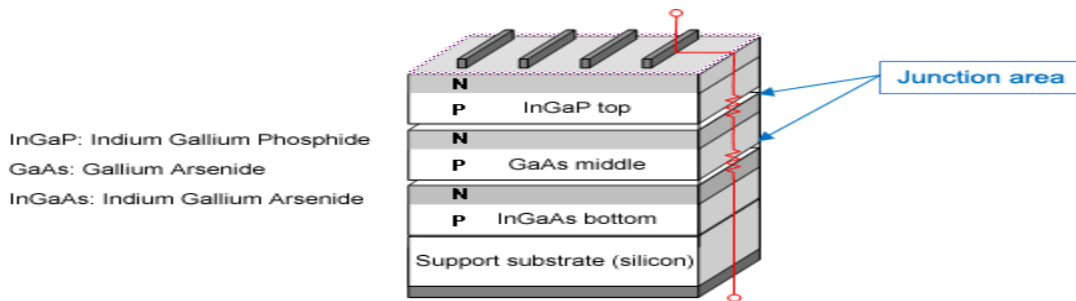


Figure I- 10: Compounds of group III-V cell structure diagram [22].

C. Third generation solar cell technology

The third generation of photovoltaic cell technology is single-junction solar cells that can overcome the Shockley-Queisser limit of 31-41% power efficiency. C-Si solar cells (first generation) and thin film solar cells There are some limitations to achieving higher efficiencies and establishing photovoltaic technologies that meet all the conditions of the Golden Triangle. The third generation of solar cell technology includes various types of solar cells:

1. CZTS solar cells including materials CZTSe and CZTSSe (Double Junction solar cells)

Double-junction InGaP/GaAs tandem cells have 30% efficiency under AM1.5g solar spectrum illumination [23]. The U.S. National Renewable Energy Laboratory (NREL) set

a world record of 32.6% double-layer solar cell efficiency under AM1.5g solar spectrum illumination [24].

Double-junction solar cell technology forms the basis of multi-junction solar cell technology, with triple-junction and quad-junction solar cells designed to absorb most of the visible photon's incident on the solar cell. Through the development of new materials and various sustainable designs of solar cells, efficiency increases by an absolute 1% per year [25].

Triple-junction solar cells: The theoretical efficiency of multi-junction solar cells can reach 86% [26], in which unlimited number of junctions can be stacked in the solar cell. Multijunction solar cells have been successfully developed using compound semiconductors. The three cells in a three-terminal solar cell absorb different parts of the incident solar spectrum. The highest efficiency achieved so far for the ternary compound GaInP/GaInAs/Ge is approximately 39% [27]. Solar cells under high light concentration of 236 suns [28].

The figure I-11 shows Schematic of Multi junction solar cell.

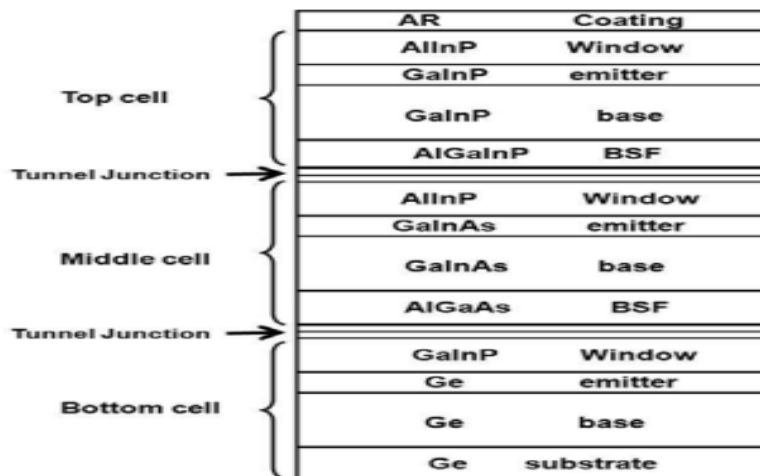


Figure I- 11: Schematic of Multi junction solar cell [29].

2. Dye sensitized solar cells

The first DSSC was developed by Michel Gratzel at the Swiss Institute of Technology [30]. DSSC solar cells use a dye between different electrodes. Cells consist of four parts: a semiconductor electrode, a dye sensitizer, a redox mediator, and a counter electrode (carbon or Pt) [31]. Simple processing methods such as printing techniques, flexibility, transparency and low costs make DSSC attractive [32]. DSSC increases its efficiency by more than 10% due to nano-sized TiO₂ photons combined with high-visibility dyes forming visible dyes [33, 34]. DSSC degradation and safety concerns are some of the problems caused by different strains [32].

3. Quantum Dot solar cells

Quantum Dot solar cells are made using tiny particles called quantum dots (a few nanometers in size) to absorb solar photons for photovoltaic purposes. Quantum dots (QDs) are tiny semiconductor particles a few nanometers in size that have optical and electronic properties that are very different from many other materials [35].

4. Perovskite solar cells

Perovskite solar cells are a new group developed by the Solar Research Group and have many advantages over simple solar cells and traditional silicon. Perovskite is a class of substances defined by the formula ABX₃; where X represents halogen such as I-, Br-, Cl- and A and B are the corresponding cations. first reported that perovskite solar cells had conversion efficiency (PCE) of up to 9.7% [36]. Durability and longevity are some of the issues of such perovskite solar cells. Performance decreases due to deterioration of the materials used in this cell [37].

The figure I-12 shows Crystal structure of organometal perovskite.

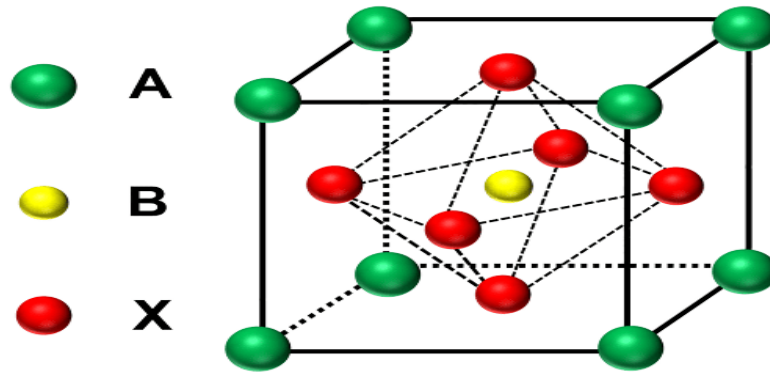


Figure I- 12: Crystal structure of organometal perovskite [38].

5. Organic solar cells

Organic solar is considered a new technology based on dyes and their physical and particularly optical properties [15].

The **figure I-13** shows Diagram of the structure of organic solar cells.

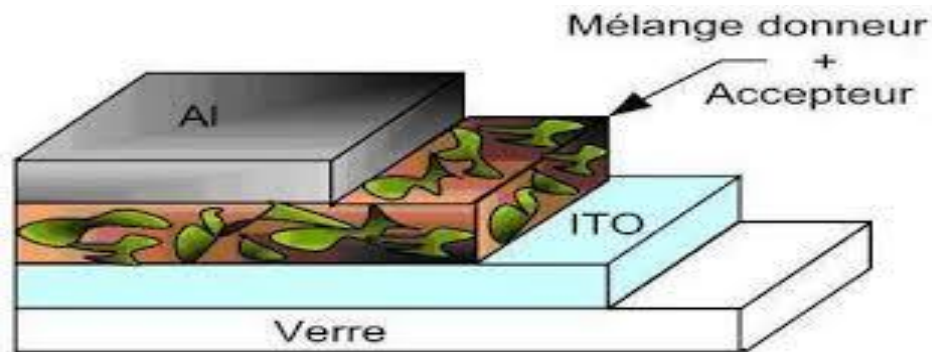


Figure I- 13: Diagram of the structure of organic solar cells [39].

I.3.4. The solar cell photovoltaic features

The **figure I-14** shows the maximum power point of the solar cell, which allows us to deduce the photovoltaic parameters of the cell:

- ❖ The short circuit current (obtained for $V=0$).
- ❖ The open circuit voltage (obtained for $I=0$).
- ❖ The form factor FF .
- ❖ Conversion efficiency.

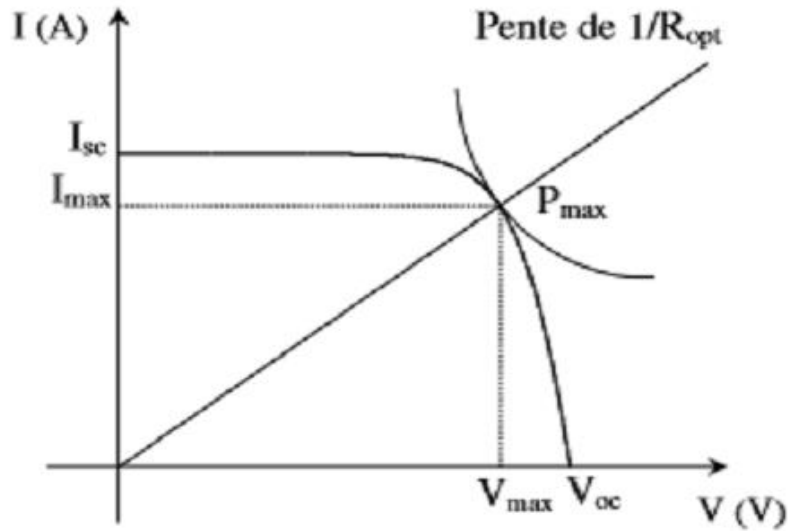


Figure I- 14: Maximum power point of an elementary cell [40].

a. The short circuit current I_{sc}

Short circuit current is the current that flows in a cell subjected to a flow of photons without any voltage applied ($V=0$). It increases linearly with the illumination intensity of the cell and depends on the illumination surface, radiation wavelength, carrier mobility and temperature. It is measured by connecting the cell terminals directly to an ammeter [40].

b. The voltage of the circuit-ouverte V_{co}

If we place a photocell without a receiver under a constant light source, we obtain a DC voltage at its connections, the so-called open circuit voltage (obtained when $I=0$).

For a unit cell, this voltage is typically around 0.5 to 0.7 V (depending on material, technology, and lighting). It represents the number of carriers generated per incident photon [40].

c. The maximum power P_m

The maximum output power of a photovoltaic cell is an important parameter for evaluating its performance; it is given by the following relationship:

$$P_m = I_m \cdot V_m \text{ [W]} \quad (1)$$

It translates on the I-V characteristic the operating point $P_m (V_m, I_m)$ which is located at the elbow of the I-V characteristic, it is called maximum power point where the values of voltage V_m and current I_m also called maximum voltage and current respectively [40].

d. The form factor FF

Shape factor is a parameter that characterizes the quality of a cell; it is defined by the ratio of maximum generated power to optimized power.

$$FF = \frac{P_m}{I_{sc} \times V_{co}} = \frac{I_m \times V_m}{I_{sc} \times V_{co}} \quad (2)$$

e. The yield η

This is the external power conversion energy efficiency. It is defined by the following relationship:

$$\eta = \frac{P_m}{G \times S} = \frac{I_m \times V_m}{G \times S} = \frac{FF \times I_{sc} \times V_{co}}{G \times S} \quad (3)$$

G: Irradiation power [W/m^2].

S: Surface of the photovoltaic cell [m^2].

P_m : Maximum power [W].

I_m : The maximum current [A].

V_m : The maximum voltage [V].

FF: The form factor.

I_{sc} : The short circuit current [A].

V_{co} : The open circuit voltage [V].

This efficiency can be optimized by increasing the form factor, short circuit current and open circuit voltage. It is an essential parameter, because just knowing its value makes it possible to evaluate the performance of the cell [40].

I.3.5. Assembly of solar cells (series, parallel, series-parallel)

A. Serial association

In a series connection, the cells carry the same current, and the final characteristics of the series connection are obtained by adding voltage at a certain current. **Figure I-15** shows the characterization results obtained by connecting identical cells in series [41].

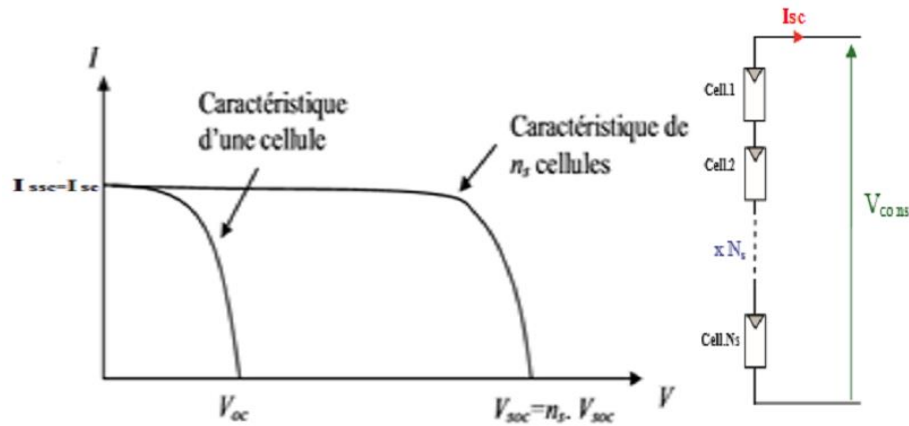


Figure I- 15: Features derived by sequentially grouping rows of the same cells [42].

B. Parallel association

cells grouped in parallel have twice the performance of cells grouped in series. Thus, in a group of cells connected in parallel, the cells are exposed to the same voltage, and the final characteristics of the group are obtained by adding current at a specific voltage. **Figure I-16** shows the resulting characteristics obtained by connecting n_p identical cells in parallel [41].

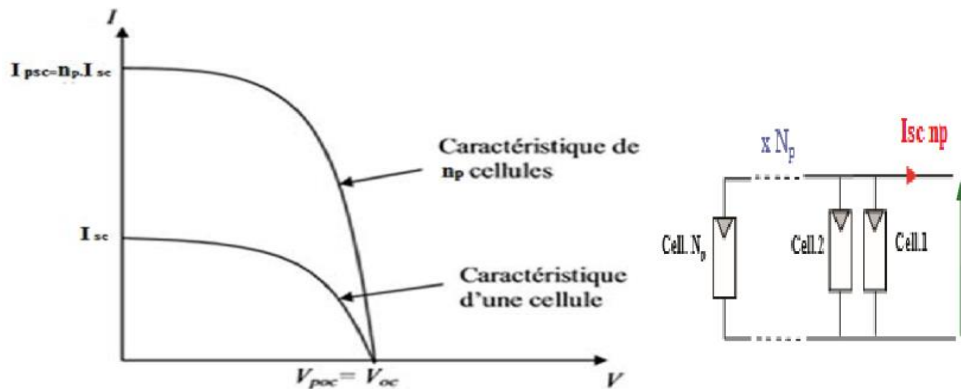


Figure I- 16: Features derived by grouping rows on branches of the same cells [42].

C. Hybrid association (series/parallel)

Depending on the series and/or parallel association of these cells (**figure I-17**), the values of the total short-circuit current and the total open-circuit voltage are given by the relations [41]:

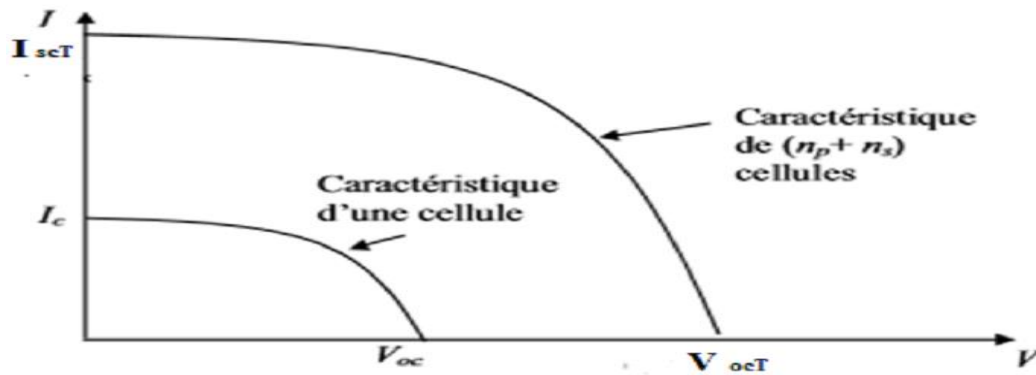


Figure I- 17: Features derived by grouping rows on a sequence and branching, from the same cells [41].

$$I_{scT} = n_p \cdot I_{cc} \quad [A] \quad (4)$$

$$V_{ocT} = n_s \cdot V_{co} \quad [V] \quad (5)$$

I_{sc} : Short-circuit current.

V_{oc} : Open-circuit voltage.

I_{ccT} : Total short-circuit current.

V_{coT} : Total open-circuit voltage.

I.3.6. Photovoltaic applications

Solar PV applications are diverse and different, and can be classified into two main parts
Collections:

- Autonomous systems (Isolated installations).
- Grid-connected systems (Installations connected to the network).

A. Autonomous systems (Isolated installations)

Autonomous photovoltaic systems are so-called "off-grid systems" designed to meet energy needs from the sun through photovoltaic conversion without the need to be connected to the grid. In most cases, these systems are deployed in isolated locations [43]. Photovoltaic solar energy has a variety of applications, from small calculators to satellites. The main photovoltaic energy applications in autonomous systems can be divided into the following categories: building and house electrification (BIPV), autonomous lighting, water pumping and treatment, agricultural applications, communications and many other specific applications [44]. **Figure I-18** shows the various subsystems present in an autonomous photovoltaic system.

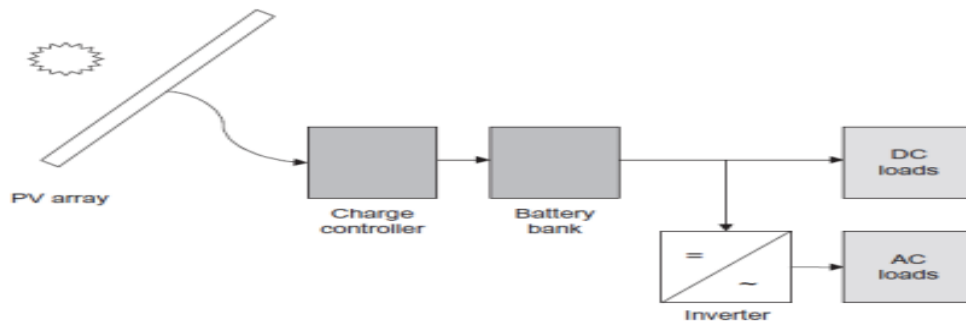


Figure I- 18: Schematic of a stand-alone PV system [45].

B. Grid-connected systems

A grid-tied PV system, also known as an "on-grid system," is a type of installation consisting of three main components: photovoltaic modules, (DC/AC) inverters, and power lines. In this type of system, the power generated by the modules is transferred directly to a (DC/AC) inverter, which converts the DC power into AC power in order to feed the generated energy into the grid [46, 47]. **Figure I-19** shows the various subsystems present in an "a grid connected PV system".

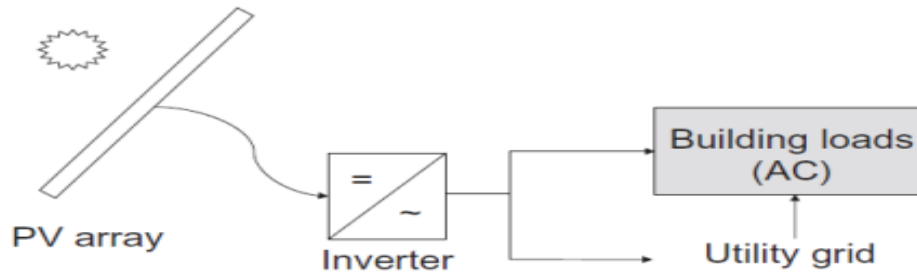


Figure I- 19: Schematic diagram of a grid connected PV system [45].

I.4. Conclusion

This chapter provides an overview of photovoltaic energy. Global photovoltaic potential, installed capacity and generation share along with important photovoltaic technologies, various photovoltaic cell parameters and photovoltaic applications are discussed. Photovoltaics has seen the highest increase in its share of electricity generation among all renewable energy sources, driven by a sharp decline in the price of photovoltaic technology.

Photovoltaic cell technology is mainly divided into three generations: silicon-based photovoltaic cells, thin-film photovoltaic cells, and other emerging technologies such as organic and perovskite photovoltaic cells. Photovoltaic energy can be used in a variety of applications and can be divided into two main categories: stand-alone PV systems (such as building electrification and water pumping) and grid-connected PV systems.

Chapter II Literature review of the PV cooling
methods and systems by geothermal energy

II.1. Introduction

Photovoltaic solar cells are greatly affected by the surrounding environmental condition and factors. This limits their efficiency and shortens their lifespan.

A sharp rise in ambient temperature is a negative impact factor on the conversion of photovoltaic cells. Therefore, researchers resort to different cooling methods and techniques to reduce the temperature of photovoltaic cells.

In this chapter, we discuss the influence of different environmental factors, with an emphasis on the influence of temperature. We also review previous studies on the PV cooling methods and systems by geothermal energy.

II.2. Environmental parameters affecting photovoltaic cells efficiency

II.2.1. Effect of radiation intensity

The radiation received by the photovoltaic cell directly affects the electrical energy produced by the photovoltaic cell. The intensity of solar radiation varies during the daylight hours, such that it usually reaches its maximum value in the middle of the day. We obtain the highest levels of solar radiation if the photovoltaic cell is oriented perpendicular to the sunlight [48]. The effect of solar radiation on the photovoltaic cell is presented shows in

Figure II-1:

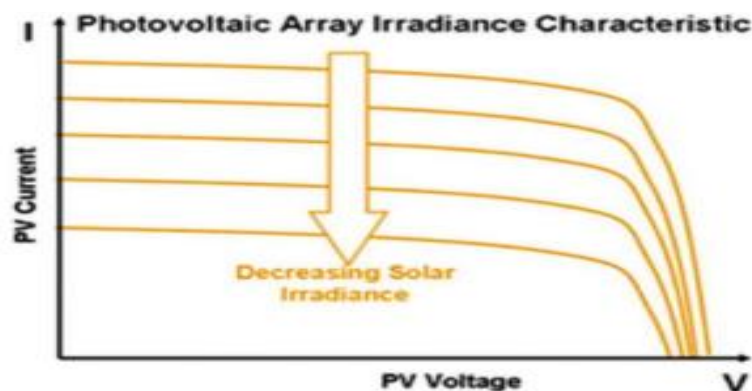


Figure II- 1: Characteristics of a solar P·V.: Effect of solar irradiance [1].

II.2.2. Temperature effect

An increase in the ambient temperature and the intensity of solar radiation results in an increase in the temperature of the photovoltaic cell [49]. Semiconductors are the main

component of photovoltaic cells. Due to its natural characteristics. The increase in temperature leads to a decrease in efficiency. The degradation in efficiency is caused directly by the drop in open circuit voltage as the cell temperature rises. Based on a review of the previous study, the efficiency of the crystalline cell decreases by 0.5% for every 1°C increase in the temperature of the photovoltaic cell [48]. **Figure II-2** represents the effect of temperature on the photovoltaic cell:

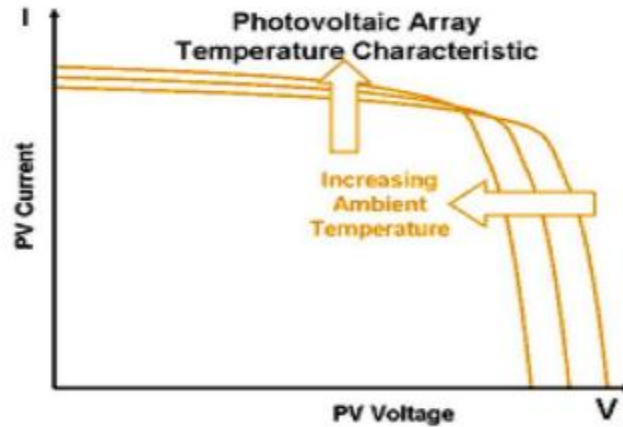


Figure II- 2: Characteristics of a solar P·V.: Effect of solar temperature [1].

II.2.3.Wind effect

Wind speed plays a major role in photovoltaic energy generation. When wind flows, the temperature of the photovoltaic cell decreases [50]. The wind cools the photovoltaic cell, causing the electrons to vibrate less, enabling the electrons to carry more energy as they move to a higher state. A photovoltaic cell cooled by 1°C is 0.05% more efficient.

II.2.4.Dust effect

Dust partially blocks solar radiation, causing a decrease in the amount of sunlight received and thus affecting the production of the photovoltaic cell. The presence of dust on the surface of the photovoltaic cell leads to a deterioration in the cell's production rate by approximately 7% [48].

II.2.5.Shading effect

Shading causes degradation and a significant decrease in the efficiency of photovoltaic cells. The shade affects the current inside the cells as well as on the plate due to the cells being connected in series.

A photovoltaic unit shaded by 2% produces approximately 70% less electricity, which indicates the significant impact of shading on the efficiency of photovoltaic cells [51].

II.2.6. Humidity effect

The presence of moisture accelerates the deterioration of photovoltaic cells [52]. Humidity prevents the cell from fully absorbing sunlight. When the humidity is very high, a layer of water vapor forms on the surface of the photovoltaic cell facing the sunlight. This layer causes a partial loss of the receiving energy due to the absorption and reflection of solar radiation due to this layer [53].

II.3. Literature review the PV cooling methods and systems by geothermal energy

Many studies have dealt with geothermal photovoltaic cooling systems, and for this we analyzed the different approaches encountered in the literature, to find out the results of the main topics that are implemented in the same field of geothermal energy in general. This analysis forms an interesting basis for work before designing the model.

The synthesis of the main approaches encountered in the literature made it possible to develop the main lines of the basic work developed. Among these studies we mention:

Sahay et al [54]. reported on a newly developed approach called the Ground-Coupled Central Panel Cooling System (GC-CPCS). The proposed system aims to cool solar panels by forced convection of air driven by a fan powered by another dedicated photovoltaic panel. The air flows through a ground-coupled heat exchanger and reduces its temperature. The cooled air calms the solar panels as it flows under them. The researchers installed nine solar panels, each with a power of 100W, and the air was circulated by a single fan, with the cool air distributed to each solar panel through ducts. Nozzles were attached to the ducts to ensure that the air flows in the desired direction. The authors reported that the use of GC-CPCS resulted in a significant increase in conversion efficiency. **Figure II-3** shows Schematic design of ground coupled-central panel cooling system (GC-CPCS).

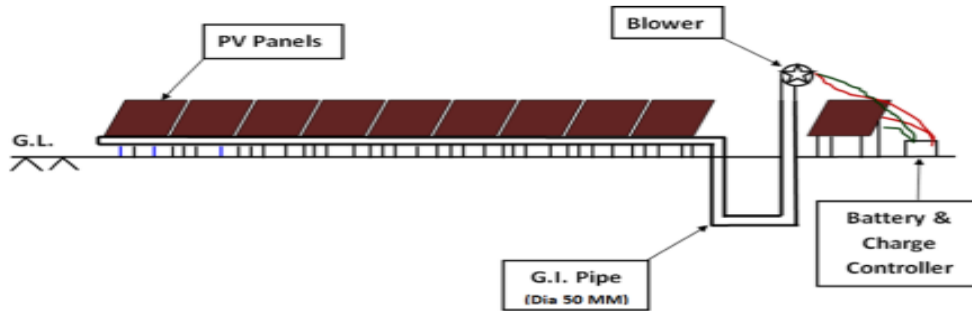


Figure II- 3: Schematic design of ground coupled-central panel cooling system (GC-CPCS) [54].

In a study by Elminshawy et al [55]. An underground heat exchanger was used for air precooling. A schematic diagram of their experimental setup is shown in **Figure II-4**. In their study, various elevated ambient air temperatures of 35°C, 40°C, and 45°C were tested along with different flow rates to evaluate their impact on module efficiency. It was observed that the temperature could be effectively regulated by using a heat exchanger. The comparison of panel output power showed that the daily electrical efficiency was improved by up to 29.11% with this cooling method. **Figure II-4** shows Schematic of PV air cooling with buried heat exchanger.

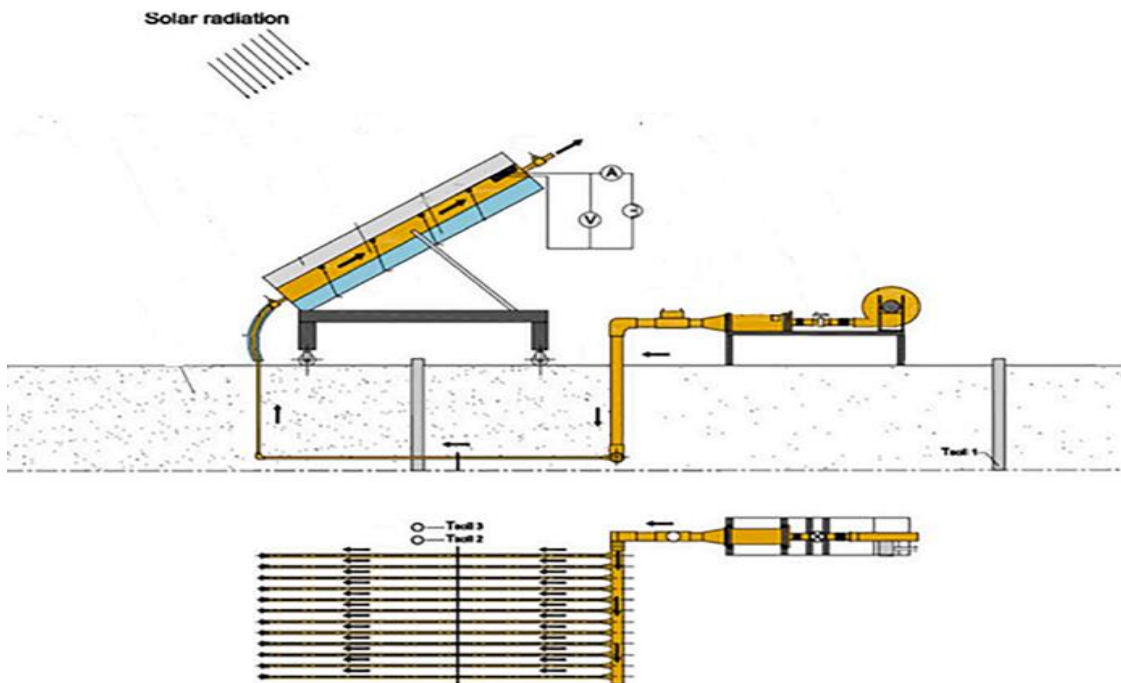


Figure II- 4: Schematic of PV air cooling with buried heat exchanger [55].

Elminshawy et al [56]. A new alternative cooling system for PV panels, involving the passage of pre-cooled outdoor air over the backside of the PV panels, was experimentally studied under local conditions in Port Said, Egypt. This alternative cooling system employs an earth-air heat exchanger (EAHE) to simultaneously improve PV panel performance by first pre-cooling the outdoor air and then cooling the backside of the PV panels. by pre-cooling the backside of the PV modules with geothermal heat at an optimal flow rate of 0.0288 m³/s, the PV module temperature could be reduced from an average of 55°C (without cooling) to 42°C. At this optimal flow rate, the PV module output increased by an average of about 18.90% and the electrical efficiency by an average of about 22.98% due to the PV module temperature reduction. According to the economic evaluation, the proposed cooling system improved the relative levelized energy cost by 12% and avoided approximately 13896 g of CO₂ emissions during the summer season.

D. Lopez-Pascual et al [57]. A compact cooling system for commercial photovoltaic panels based on low-enthalpy geothermal cooling is proposed. A single-phase, closed-loop cooling system that benefits from a natural underground heat sink at a constant low temperature to exhaust superheat from the solar panels. A prototype incorporating a single-axis solar tracking mechanism was assembled and tested outdoors in Alcalá de Henares, Madrid, Spain, in June 2022. The results showed that a cooling water flow rate of 1.8 liters/minute per square meter of panel surface reduced the temperature of the cooled panels to 20°C and improved the efficiency of the panels to 13.8%.

Kadhim and Aljubury [58]. In this study, an experimental prototype was fabricated to investigate the use of an underground water tank as a heat exchange medium with the soil to reduce the operating temperature of photovoltaic (PV) panels and simultaneously improve PV efficiency. Three PV systems were evaluated: benchmark PV panels without cooling (Panel A), PV panels with sprinkling PV panel with cooling (Panel B), and a PV panel with evaporative cooling (Panel C). The cooling techniques for modules (B) and (C) were used to investigate the influence of groundwater on the performance of the PV panels under dry conditions. Four cases were devised: rear cooling with spray panels (I), front and rear cooling with spray (II), front and rear cooling with spray using an Arduino controller (III), and repeating case III with different water flow rates (IV). Measurements were taken

from May to August, from 9 am to 4 pm. Experimental results showed that when groundwater spray cooling was used, the temperature of PV panel B decreased by 14°C, 17.6°C, 18.8°C, and 22.7°C in cases I, II, III, and IV, respectively, compared to the uncooled panel, and the efficiency increased by 3.5%, 4.8%, 18%, and 23.1%, respectively.

Figure II-5 shows schematic diagram of the experimental setup.

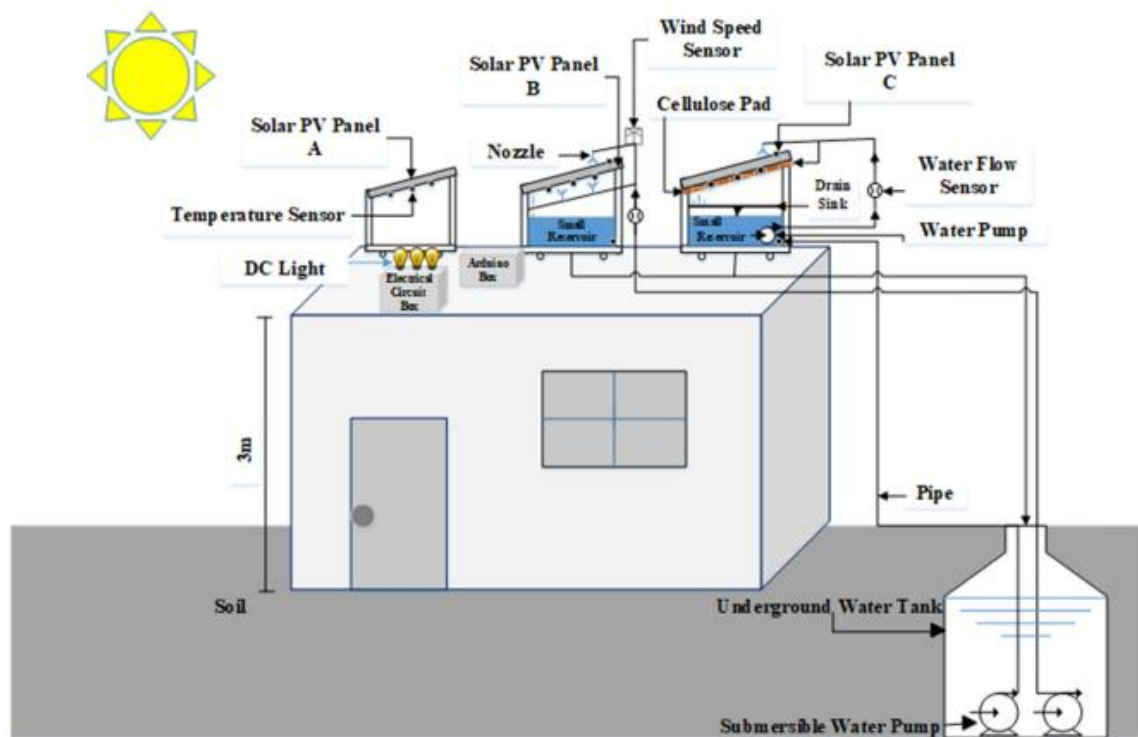


Figure II- 5:A schematic diagram of the experimental setup [58].

Li-Hao Yang et al [59]. In this study, a cooling system using shallow geothermal heat was experimentally investigated to mitigate the problem of low conversion efficiency of solar panels, and a mathematical model was developed to predict system performance. The cooling system cools the panels by spraying water on the backside of the panels, which is then returned to the tank. To increase the cooling capacity, the recycled water is collected in a U-shaped borehole heat exchanger (UBHE) installed in an existing well to exchange heat with shallow geothermal energy. Finally, the panels will be sprayed with water again for cooling. The experiment consisted of three phases: the first phase consisted of operating the panels without a cooling system; the second phase consisted of using a cooling system without a UBHE; the third phase consisted of using a cooling system with a UBHE. The

experimental results and the mathematical model show the same trend: cooling systems can increase the conversion efficiency of the panels, and furthermore, as the temperature and the number of panels increase, the benefits become obvious. For example, in a plant factory powered by panels, the cooling system can increase efficiency by 14.3%, and the capital cost can be recovered in 8.7 years by this system. **Figure II-6** shows the schematic diagram of the system.

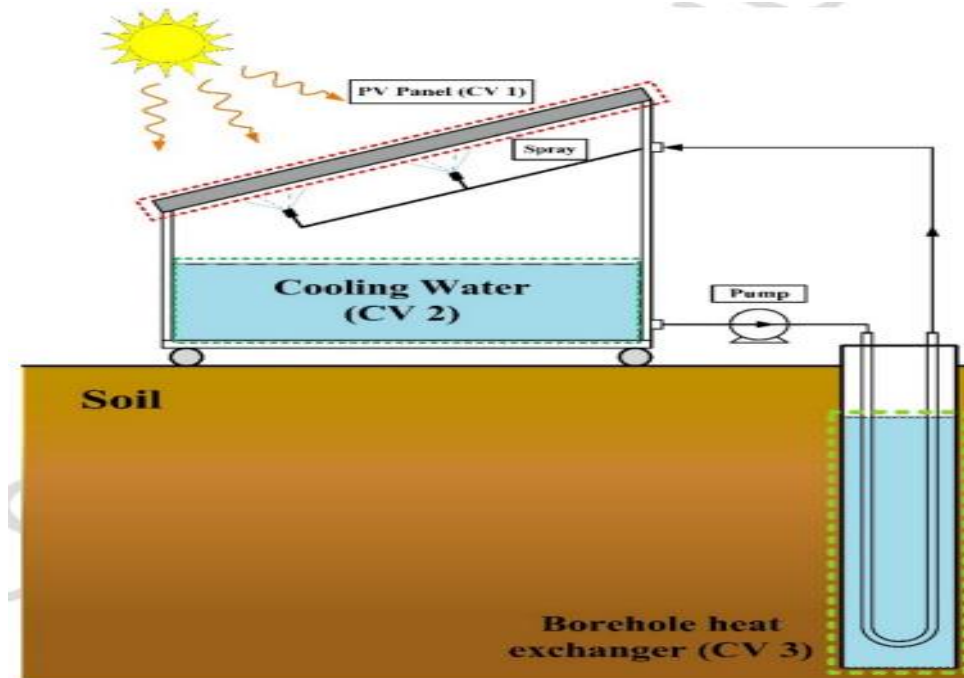


Figure II- 6: the schematic diagram of the system [59].

R. Jafari [60]. In this study, cooling water (water + ethylene glycol) is circulated between two heat exchangers. The mini-channel heat exchanger is in contact with the solar cells, while the geothermal heat exchanger is buried underground and set up to take heat from the solar cells to the ground. Six control factors of the geothermal cooling system were considered for optimization using Taguchi design and main effects analysis. These parameters were pipe length, soil thermal conductivity, cooling water flow rate, distance between adjacent coils, pipe inner diameter, and pipe thickness. Experimental results showed that the average power production of the cooled PV panels was 9.8% higher than that of the PV panels without the cooling system. However, when the same geothermal heat exchanger is used, the amount of electricity generated drops to 6.2% when the number of

cooled panels is doubled. Simulation results show that the optimal configuration of the geothermal cooling system can improve the net power generation of the twin cooling panels by up to 11.6%. The LCOE of the optimized geothermal cooling system is 0.089 Euro/kWh, compared to 0.102 Euro/kWh for the 30 kW PV power plant case study.

Figure II-7 shows Schematic connections of the designed PV panel with cooling system.

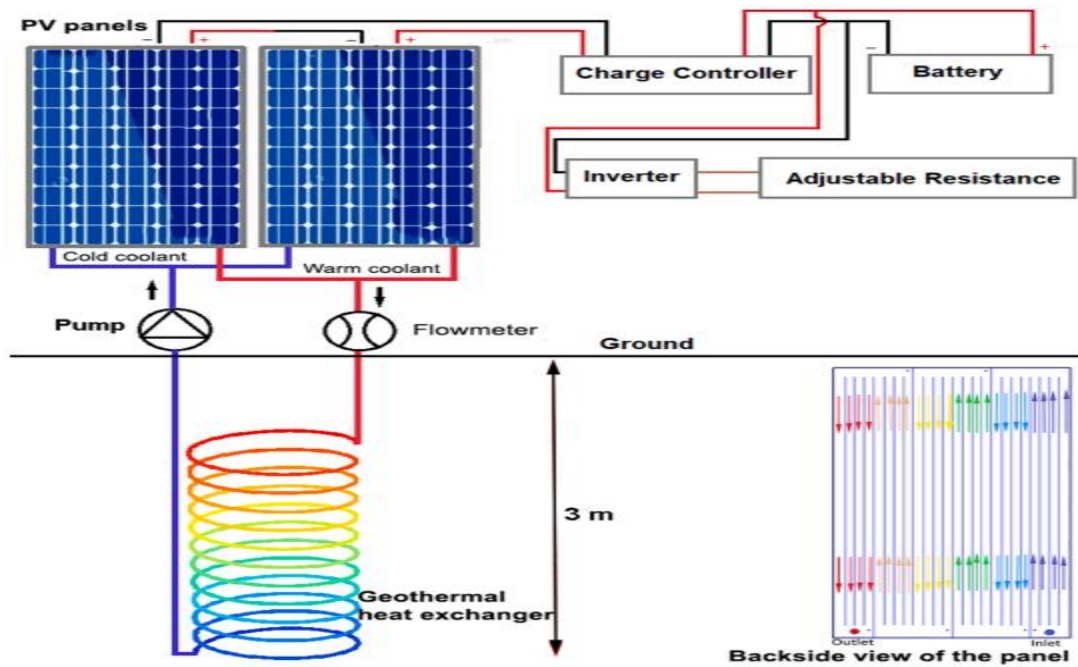


Figure II- 7:Schematic connections of the designed PV panel with cooling system [60].

Y. Ruoping et al [61]. This study proposes a photovoltaic power generation system with ground heat exchangers (PV-GHEs system). Taking Tikanlik, a typical arid climate in northwest China, as an example, a numerical model based on TRNSYS software is constructed and its reliability is verified based on actual thermal response test data. Simulation results showed that the PV-GHEs system reduced panel temperature by 26.8% and increased annual power production by 7.9% compared to conventional PV systems.

Figure II-8 shows Schematic diagram of a simplified PV-GHEs system.

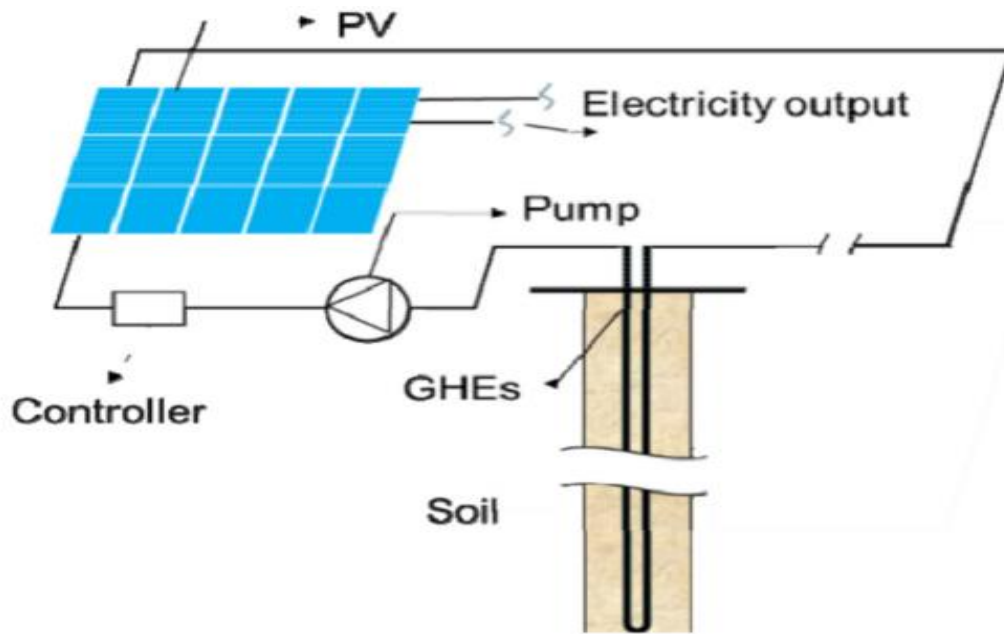


Figure II- 8: Schematic diagram of a simplified PV-GHEs system [61].

II.4. Conclusion

This chapter provides an overview of a research study investigating how different environmental factors affect the performance of photovoltaics. It is clear that climatic conditions, such as radiation intensity, dust accumulation, and ambient temperature, play a crucial role in determining the efficiency of PV systems. High ambient temperatures are particularly important, because they can reduce the efficiency of PV systems due to increased operating temperatures. This can lead to a significant decrease in the efficiency of photovoltaic cells and potentially long-term damage, ultimately shortening their lifespan. Various methods have been explored to address this problem, as geothermal cooling techniques have proven effective through results obtained from previous experiments, research and studies.

Chapter III Methodology and Experimental study
of the PV cooling system by geothermal energy

III.1. Introduction

The hot and dry weather experienced in southern Algeria, especially in summer, causes average maximum temperatures to sometimes reach 50°C in the afternoon [62].

When photovoltaic systems convert only a small portion of the incident sunlight into electrical energy, and the rest into heat, this situation is puzzling. An increase in the temperature of a photovoltaic cell significantly reduces efficiency by approximately 0.5% for each degree Celsius increase in temperature. It therefore becomes necessary to keep the temperature of the PV module low to increase efficiency and reduce thermal impact [63].

Summer usually begins in the Ouargla region in May and continues until October, when the maximum temperature ranges between 48 and 25 degrees Celsius, which raises astonishment and astonishment [62].

The main objective of this chapter is to study the geothermal cooling system that relies on air emitted from pipes buried in the ground at a specific depth to solve the problem of high temperature of the photovoltaic module by improving the conversion efficiency by reducing the operating temperature and maintaining a uniform temperature distribution. Over the PV module. The proposed geothermal cooling system was studied experimentally under real outdoor conditions during the days of May in a hot and dry area (Ouargla, southern Algeria). The thermal and electrical properties of the used PV modules (with and without cooling) were determined.

III.2. Place of the conduct the experiments

The experiments were conducted in May 2024, in 25 May from 9:20 to 11:00 hours, under the external environmental conditions of Ouargla Province, Algeria. Ouargla is characterized by a high intensity of solar radiation, a large number of clear sunny days, and a long duration of daily solar radiation, making it one of the best areas for photovoltaic energy. However, it is considered one of the hottest regions in the world (often exceeding 45°C in summer) **Figure III-1**, which poses a major challenge for photovoltaics. On July 5, 2018, the highest global temperature was recorded in the Ouargla region. Highest in Africa. Which reached 51.3 degrees Celsius. The Ouargla region is also characterized by low rainfall and relatively low humidity, and the average wind speed reaches 3.70 m/s [64].

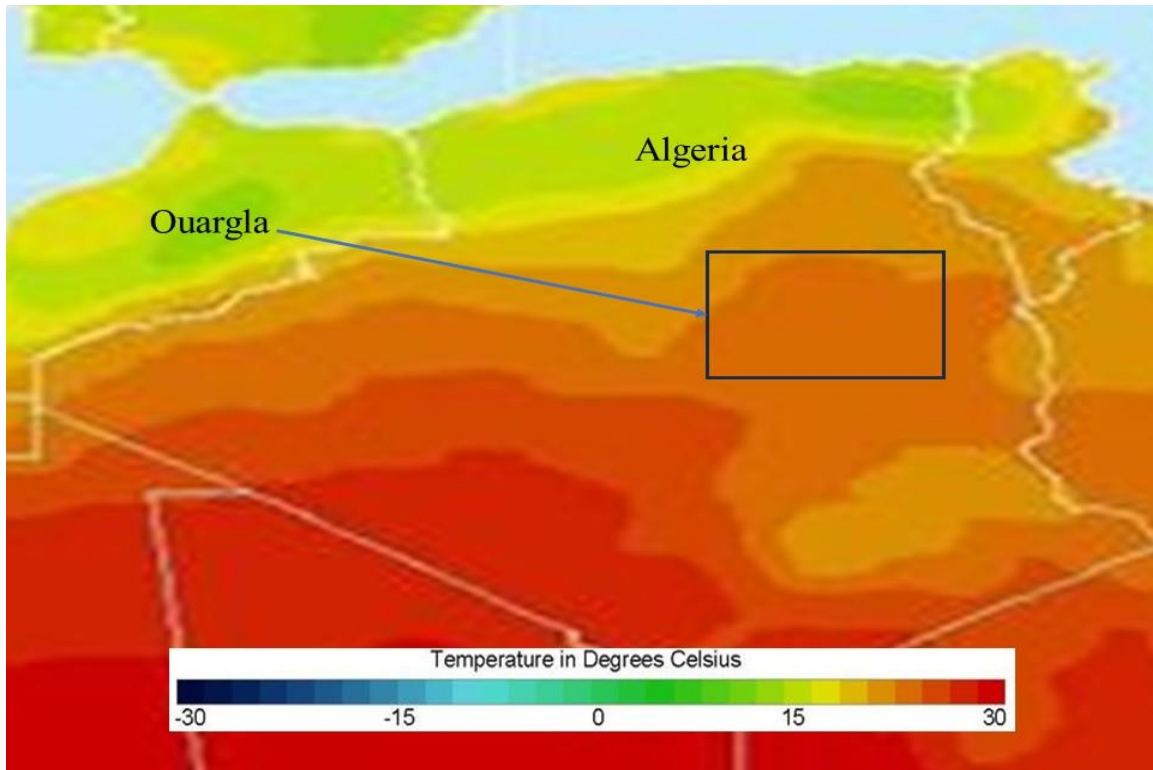


Figure III- 1: Average annual temperature for Algeria, and Ouargla State [65].

III.3. Description of the experimental device

As is known, geothermal cooling is considered a potential solution to the temperature problem of photovoltaic modules. From a certain depth, the temperature below the surface is constant throughout the year. Subsurface temperatures range between 10°C and 20°C at shallow depths ranging from 5 to 15 meters [57].

In the experimental system, the system created by the research team in fuels and energy transfer within the framework of the doctoral thesis of the student Ben Ali Oussama, is linked to the third pole of the University of Ouargla. This system is connected to a photovoltaic cell for the purpose of cooling it, while a second photovoltaic cell remains a reference for comparison between them.

The system consists of pipes buried at a depth of 2.5 meters, through which the air needed to cool the photovoltaic modules circulates. The tubes form an S at the horizontal ground level. The pipes are made of polyvinyl chloride (PVC) and are 47 meters long and 0.11 meters in diameter, arranged separately from each other. With a distance between the

two axes of 2 meters and 3 floors. **Figure III-2** represents the system used to cool photovoltaic panels. A variable flow extractor (50-Watt portable fan) is placed at the inlet of the system to ensure continuous air circulation shown in **Figure III-4**. While the system outlet is connected to the PV module to be cooled.



Figure III- 2: A general display of the system used for the cooling of photovoltaic panels.

The experimental process of the cooling system connected with a photovoltaic module is shown in **Figure III-3**.

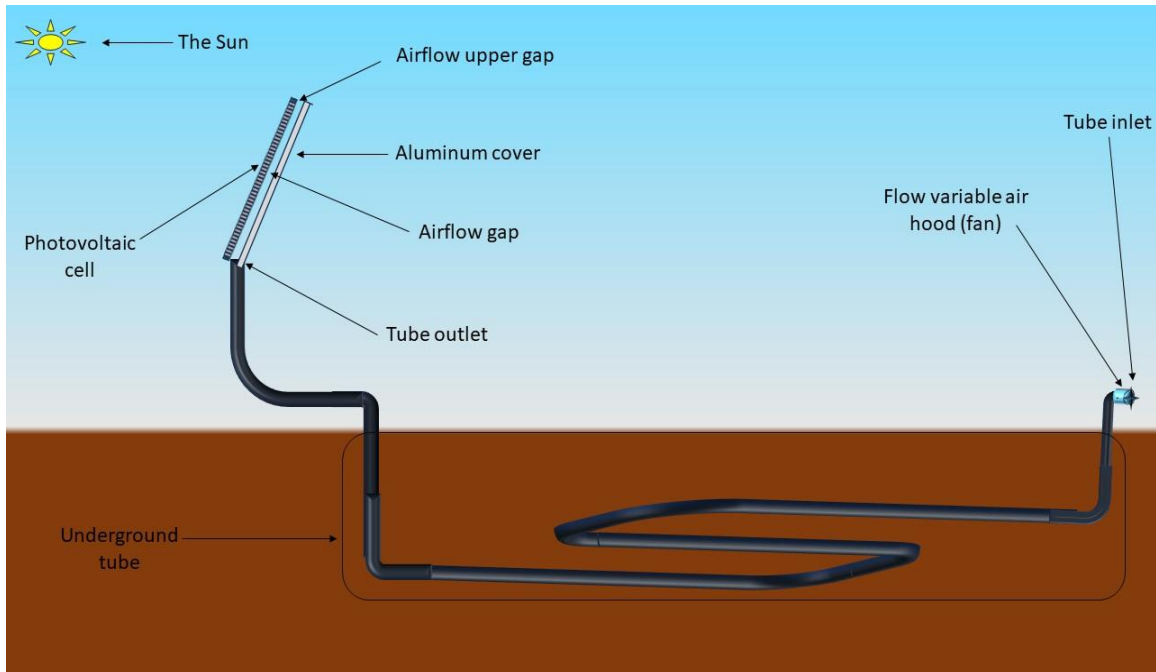


Figure III- 3: Schematic diagram of the experimental process of the cooling system.

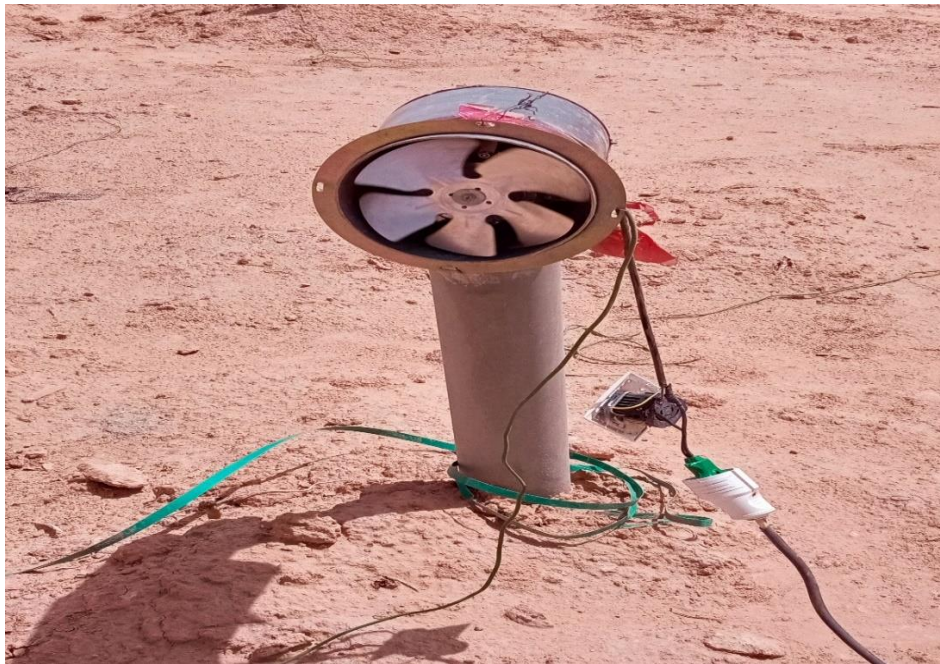


Figure III- 4: A variable flow extractor (50-Watt portable fan).

III.4. The different properties of the photovoltaic one used

Two identical polycrystalline silicon PV modules with a maximum output power of 80 W were used in this study. One unit was connected to the proposed cooling system, and the second unit was kept as a reference shown in **Figure III-7**. The units were installed next to the stadium located at the third pole of the University of Ouargla. Thus, the two units headed south with a constant inclination of latitude towards the city of Ouargla ($31^{\circ} 57'$). The experiments were conducted on May 25, 2024. **Table III-1** presents the specifications of the polycrystalline PV modules used under STC standard test conditions.

Table III-1: represents the specifications of polycrystalline PV modules used under STC standard test conditions.

Parameter	Specification
Technology	Polycrystalline
Maximum power (W)	80
Maximum voltage (V)	17.4
Maximum current (A)	4.61
Open circuit voltage (V)	22
Short circuit current (A)	4.85
Area(mm ²)	900 × 670

A rectangular, corrosion-resistant aluminum cover is installed behind a photovoltaic cell used in the experiment to create a gap for airflow flowing from the pipe buried underground. So, the tube is connected to a circular channel, and the circular channel is connected to a triangular channel up to the rectangular cover installed on the photocell to be cooled from the bottom, and to ensure continuity of air flow along the photovoltaic cell, we leave a space at the top of the photocell. The cover is shown in the **figure III-5**.

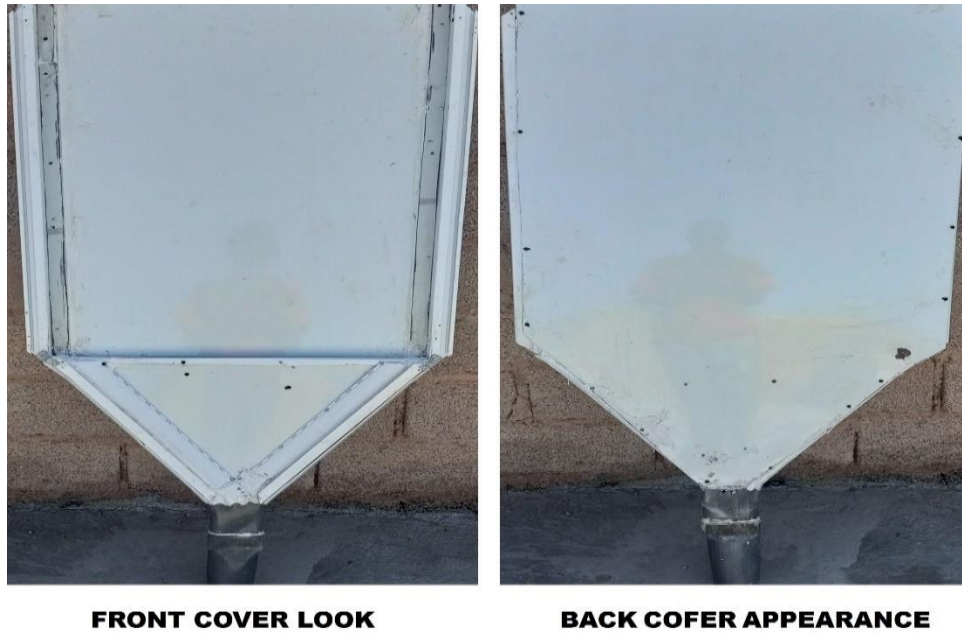


Figure III- 5: The cover used in the experimental study.

The cover and photovoltaic panel used in the experimental study are shown in the **figure III-6**, connected to each other:



Figure III- 6: The cover and connected photovoltaic panel used in the experimental study.

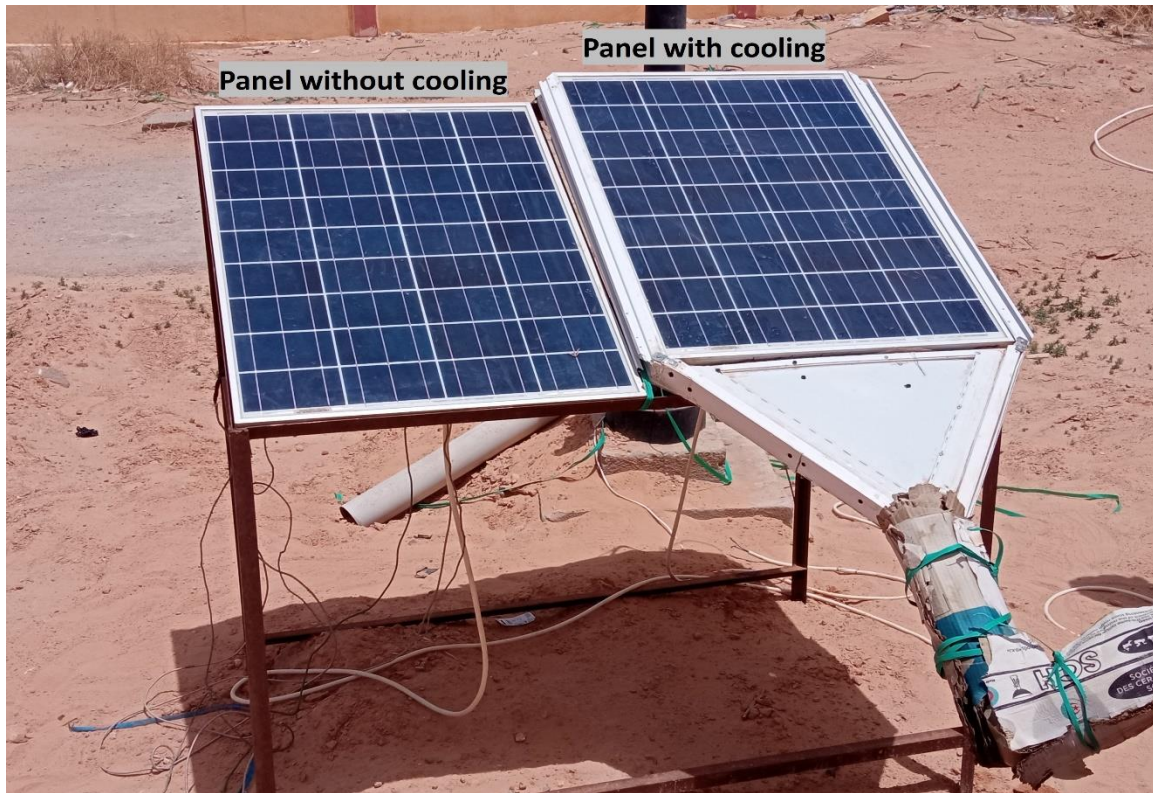


Figure III- 7: Front view of the experimental setup.

III.5. Different measurement equipment for an experiment

The thermal and electrical characteristics of both the reference and test (refrigerated) units were monitored and measured using a digital multimeter (multimeter DM750M) to measure the unit's output power in terms of voltage.


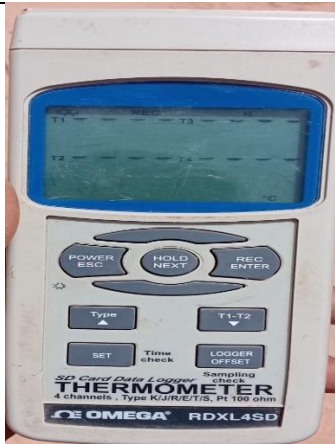
Three K-type thermocouples are positioned vertically at different positions on the back surface of each module shown in **Figure III-8**. To measure the operating temperature, a thermocouple is connected to a thermometer (Thermometer RDXL4SD).



On the test days, weather parameters such as ambient temperature, solar radiation, and wind speed were monitored and measured respectively using an anemometer, ambient temperature (mini anemometer UT363), and solar radiation intensity meter (hand pyranometer 4890.20). **Table III-2** shows details of the specifications of the various measuring devices used according to the technical data of the equipment manufacturers.



Figure III- 8: Distribution method for K-type thermocouples.

Table III-2: represents details of the specifications of the various measuring devices used according to the technical data of the equipment manufacturers.

Parameter	Instrument module	Figure	Range	Accuracy
DC - voltage (V)	multimeter DM750M		0 - 1000V	±0.5%
Temperatures (T)	Thermometer RDXL4SD		-50.1 - 1300°C	±0.4

Wind velocity and ambient temperature (Ta)	mini anemometer UT363		0 - 30m/s -10°C - 50°C	± 5% ± 2
Solar irradiation (G)	Hand pyranometer 4890.20		0 – 1999 W/m2	±5%

III.6. Results and discussions

The experimental tests were conducted in real outdoor conditions in Ouargla Province on May 25, 2024 from 9:20 to 11:00 local time.

Table III-3 and **Figure III-9** show the evolution of solar irradiation (G), and the ambient temperature (Ta) is shown in **Table III-4** and **Figure III-10**. The length of the test period. In general, the weather was sunny and the wind was light, with a speed not exceeding 2.5 meter per second. We noticed that the ambient temperature levels and solar radiation intensity were constantly increasing throughout the test period.

Table III-3: values Obtained of solar irradiation intensity (G) throughout the experimental test period.

Time	Irradiation (W/m ²)
9:20	300
9:40	437
10:00	475
10:30	510
11:00	555

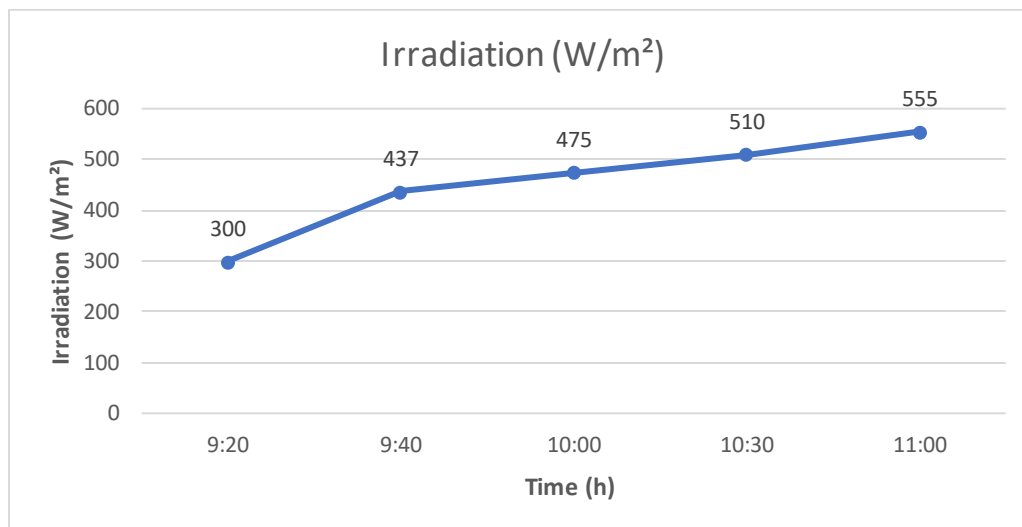


Figure III- 9: Evolution of solar radiation intensity (G) throughout the experimental test period.

Table III-4: values Obtained of ambient temperature (Ta) throughout the experimental test period.

Time	Ambient temperature (°C)
9:20	28.6
9:40	30.1
10:00	30.1
10:30	32.6
11:00	32.7

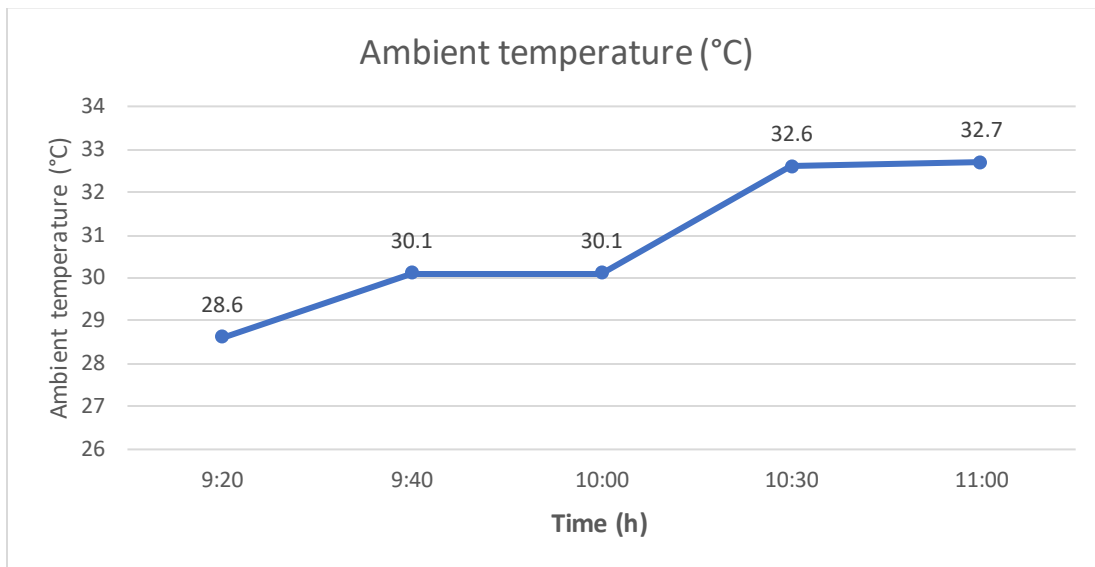


Figure III- 10: Evolution of ambient temperature (T_a) throughout the experimental test period.

The **table III-5** and **figure III-11** represent the change in wind speed with respect to time throughout the test period, so that it was noted that the wind speed was low compared to the volatile weather condition experienced by the Ouargla region in the month of May due to the strong, hottest wind blowing, known colloquially as Chehili.

Table III-5: values Obtained of wind velocity throughout the experimental test period.

Time	WIND Velocity (m/s)
9:20	1.6
9:40	1.5
10:00	1.1
10:30	1.9
11:00	2

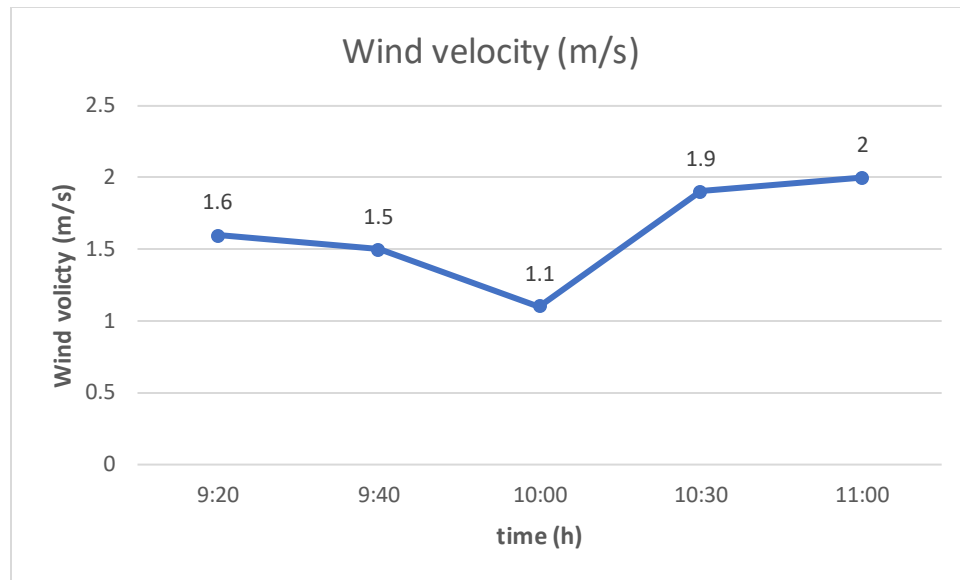


Figure III- 11: Evolution of wind velocity throughout the experimental test period.

III.6.1. Cooling effect on thermal characteristics

Studying the effect of geothermal cooling system on the thermal properties of photovoltaic cells. Three thermocouples are mounted on the back of each module (cooled plate and reference plate). The three thermocouples are mounted at different locations (bottom, middle, and top) on the back surface of the cooled and reference PV panels.

The Tc1, Tc2, Tc3, curves for the cooled plate are represented in orange and the Tr1, Tr2, Tr3, curves are represented in blue for the reference plate.

Based on the results recorded in the experiment, we note that there is a decrease in the temperature Tc1 of the cooled panel compared to the temperature Tr1 of the reference panel, as shown in the **table III-6** and **figure III-12**. This is due to the air flow from the pipe buried underground, which allows air to be transmitted from the bottom of the photovoltaic panel. To the top of the photovoltaic panel.

Table III-6: values Obtained of temperature Tc1 for the cooled and Tr1 reference PV panels for the duration of the experiment.

Time	Tr1 panel without cooling	Tc1 panel with cooling
9:20	38.9	22.1
9:40	40.5	34.6
10:00	43.6	36.9
10:30	46.7	35.6
11:00	47.3	34.3

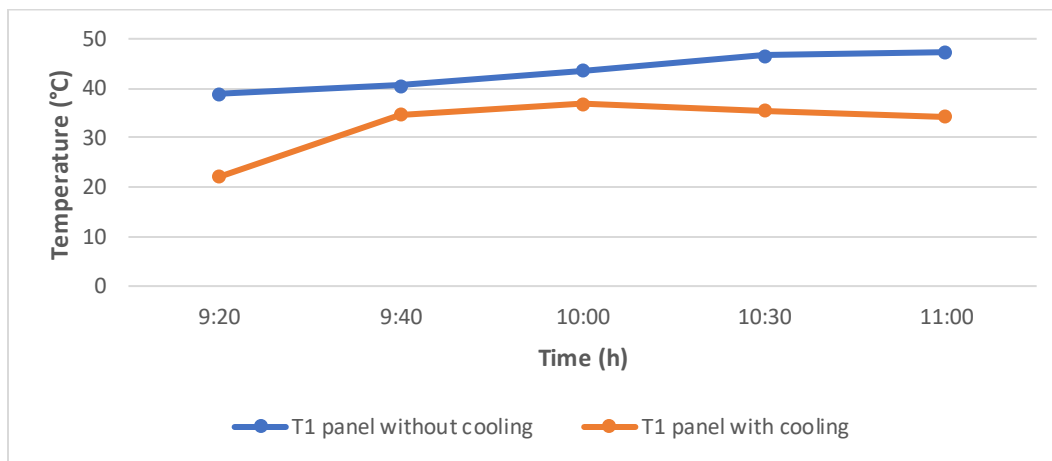


Figure III- 12: Evolution of temperature Tc1 for the cooled and Tr1 reference PV panels throughout the experimental test period.

Table III-7 and **Figure III-13** show the results obtained for the temperature Tc2 of the cooled and Tr1 reference photovoltaic panels, so that we notice a change in the temperature Tc2 of the cooled panel up and down, possibly due to the slow transfer of flowing air or measuring equipment, and the temperature Tr2 of the reference panel remains in a gradual rising state, and this Due to the concentration of direct solar radiation in the central part of the photovoltaic panel, which causes a rise in temperature in the center of the photovoltaic panel.

Table III-7: values Obtained of temperature T2 for the cooled and reference PV panels for the duration of the experiment.

Time	Tr2 panel without cooling	Tc2 panel with cooling
9:20	41	37
9:40	43	45.6
10:00	46.6	38
10:30	49	48.2
11:00	50.1	44.9

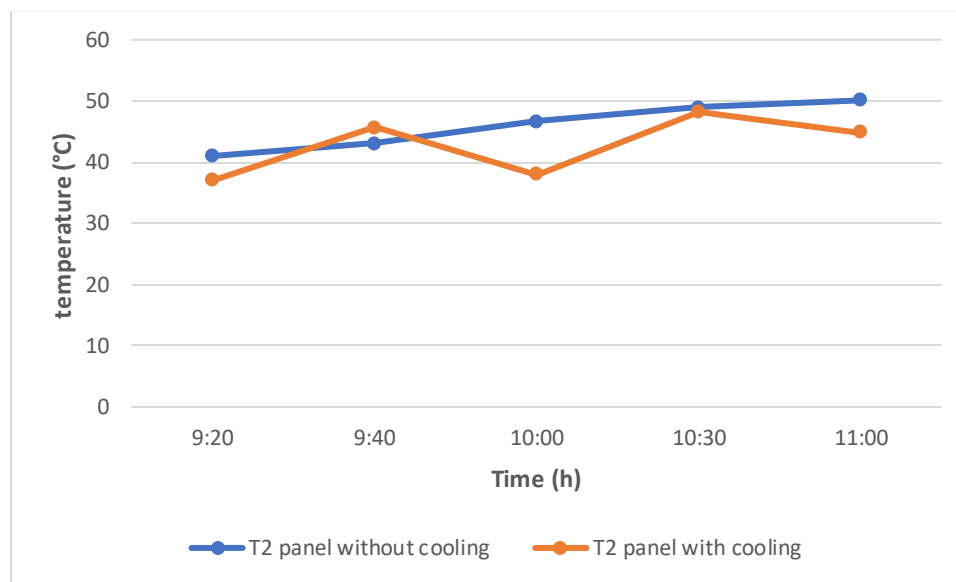
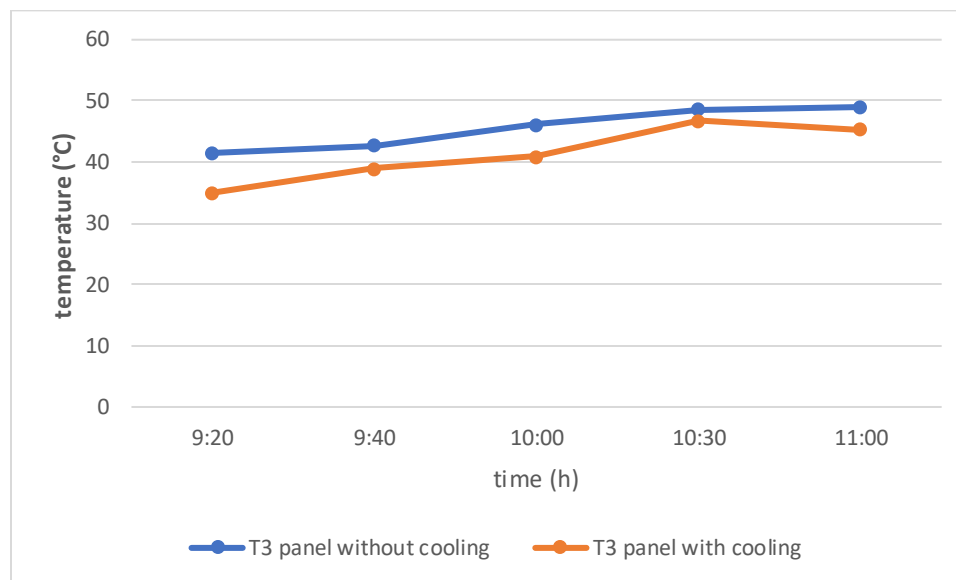
**Figure III- 13:** Evolution of temperature Tc2 for the cooled and Tr2 reference PV panels throughout the experimental test period.

Table III-8 and **Figure III-14** show the results obtained for temperature Tc3 of the cooled PV panel and Tr3 of the reference PV panel.

Therefore, we notice a gradual increase in temperature in both panels, but there is a slight difference in the temperature values between the two panels. We also note that the temperature values in the reference photovoltaic panel are slightly higher than the values of the cooled photovoltaic panel.

Table III-8: values Obtained of temperature T3 for the cooled and reference PV panels for the duration of the experiment.

Time	Tr3 panel without cooling	Tc3 panel with cooling
9:20	41.5	35
9:40	42.7	39
10:00	46.2	41
10:30	48.6	46.8
11:00	49	45.3

**Figure III- 14:** Evolution of temperature Tc3 for the cooled and Tr3 reference PV panels throughout the experimental test period.

III.6.2. Cooling effect on electrical characteristics

The electrical properties of the two PV panels (with and without cooling) were measured by measuring the voltage (V) only is shown the **table III-9** and the **figure III-15**.

So, it was observed that there was no difference in the output voltage in both panels, but it is noted that the rise in temperature affected the reference photovoltaic panel, so that we notice a gradual decrease in the value of the output voltage throughout the duration of the

experiment. We notice a change in the values of the resulting voltage, going down and up in the cooled photovoltaic panel.

As a general note, not using variable resistance affected the results of the effort obtained due to the lack of availability of variable resistance.

Table III-9: values Obtained of voltage for the cooled and reference PV panels for the duration of the experiment.

Time	Voltage panel without cooling	Voltage panel with cooling
9:20	20.21	20.1
9:40	20.18	19.9
10:00	20.1	20.24
10:30	20.06	19.75
11:00	19.98	19.96

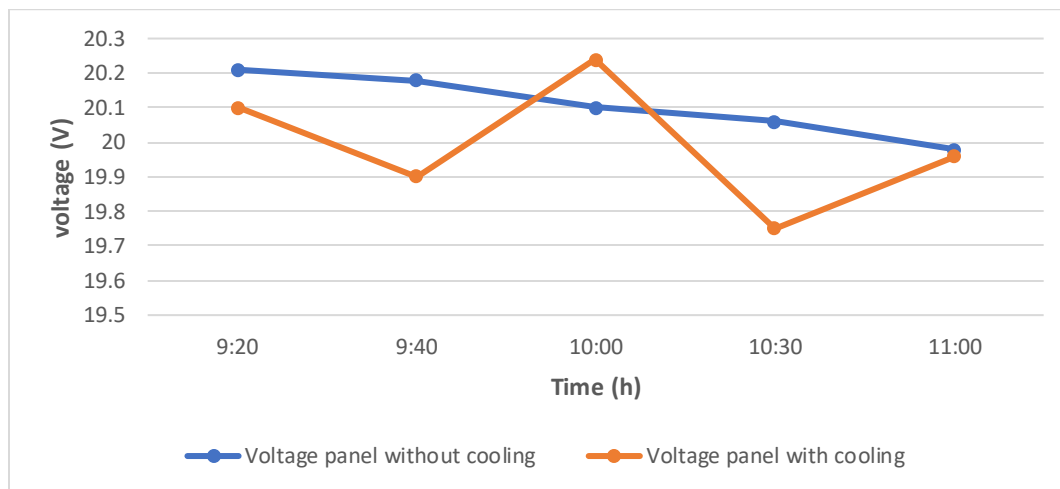


Figure III- 15: Evolution of voltage for the cooled and reference PV panels throughout the experimental test period.

General conclusion

Photovoltaics energy, also known as solar energy, is a renewable form of energy derived from the sun. This energy uses solar panels made up of photovoltaic cells to convert sunlight into electricity. These cells are responsible for capturing the sun's energy and converting it into a usable form of electricity.

Solar PV technology works by using semiconductor materials such as silicon to convert sunlight into electricity. When sunlight hits a photovoltaic solar cell, it emits electrons from the atom and generates an electric current. This electricity can be used to power homes, businesses, and even entire communities.

The use of geothermal energy can effectively cool the photovoltaic solar cells to improve their performance. By lowering the cell temperature, thermal losses are reduced and the electric efficiency of the photovoltaic panels is increased. This leads to more energy than the same cell area, which enhances the return on investment and reduces the cost of cost recovery. In addition, refrigeration techniques such as ground heat exchangers can extend the life of PV solar cells by reducing the harmful effects of excessive heat.

In this study, we aimed to investigate the improvement of photovoltaic panel efficiency using a geothermal cooling system.

The experiments led to a lowering of the temperature of the cooled plate by 6 degrees Celsius than the reference plate.

We also concluded that the speed of air flow from the pipe buried underground affects the speed of cooling of the photovoltaic panel, meaning that the faster the air flow speed increases, the faster the rate of cooling of the photovoltaic panel increases.

Experiments also showed that a gradual increase in the temperature of the photovoltaic panel that was used as a reference was offset by a gradual decrease in the voltage produced by the photovoltaic panel that was used as a reference. This confirms that if the resulting electrical voltage decreases, the power produced by the panel also decreases, and thus the efficiency decreases.

It can be said that the duration of the experiment we conducted was not sufficient to show the desired results. However, the results obtained push us to further research and development in this field, which is considered one of the important and future areas.

References

1. Dwivedi, P., et al., *Advanced cooling techniques of PV modules: A state of art*. 2020. **21**: p. 100674.
2. Krishan, O. and S.J.J.o.E.S. Suhag, *Techno-economic analysis of a hybrid renewable energy system for an energy poor rural community*. 2019. **23**: p. 305-319.
3. BELLOUFI, Y., *Etude théorique et expérimentale de l'exploitation de la géothermie dans le réchauffement ou le refroidissement d'un fluide caloporteur utilisé pour le confort thermique de l'habitat*. 2017, Université Mohamed Khider-Biskra.
4. Abdulmunem, A.R., et al., *Enhancing PV Cell's electrical efficiency using phase change material with copper foam matrix and multi-walled carbon nanotubes as passive cooling method*. 2020. **160**: p. 663-675.
5. Xu, H., et al., *Energy conversion performance of a PV/T-PCM system under different thermal regulation strategies*. 2021. **229**: p. 113660.
6. Oleksiy, N.J.I.n.d.s.a.d.L., *Simulation, fabrication et analyse de cellules photovoltaïques à contacts arrières interdigités*. 2005.
7. IEA. Available from: www.iea.org.
8. IEA-PVPS. Available from: www.iea-pvps.org.
9. Krauter, S.C.W., *Solar Electric Power Generation - Photovoltaic Energy Systems: Modeling of Optical and Thermal Performance, Electrical Yield, Energy Balance, Effect on Reduction of Greenhouse Gas Emissions*. 2007: Springer Berlin Heidelberg.
10. Hanène, M., *Modélisation et simulation du panneau solaire sous différents rayonnement*. 2021, Faculté des Sciences et Technologies.
11. Zhang, H., et al., *Photovoltaics: Reviewing the European feed-in-tariffs and changing PV efficiencies and costs*. 2014. **2014**(1): p. 404913.
12. Bernard, J.J.F., *Energie solaire calcul et optimisation Berneoud*. 2004. **106**: p. 17.
13. Ibn-Mohammed, T., et al., *Perovskite solar cells: An integrated hybrid lifecycle assessment and review in comparison with other photovoltaic technologies*. 2017. **80**: p. 1321-1344.
14. سهيلة, س., *فعالية أداء الخلايا الشمسية الكهروضوئية في ورقلة وتأثير شدة الإشعاع الشمسي و العوامل المناخية عليها*. جامعة قاصدي مرباح ورقلة.
15. Ricaud, A., *Photopiles solaires: de la physique de la conversion photovoltaïque aux filières, matériaux et procédés*. 1997: Presses polytechniques et universitaires romandes.
16. NREL. Available from: www.nrel.gov.
17. Olopade, M., O. Oyebola, and B.J.A.i.A.S.R. Adeleke, *Investigation of some materials as buffer layer in copper zinc tin sulphide (Cu₂ZnSnS₄) solar cells by SCAPS-ID*. 2012. **3**(6): p. 3396-3400.
18. Shockley, W. and H. Queisser, *Detailed balance limit of efficiency of p-n junction solar cells*, in *Renewable Energy*. 2018, Routledge. p. Vol2_35-Vol2_54.
19. Steiner, M., et al., *Optical enhancement of the open-circuit voltage in high quality GaAs solar cells*. 2013. **113**(12).
20. Schubert, M., et al., *Optical constants of Ga_xIn_{1-x}P lattice matched to GaAs*. 1995. **77**(7): p. 3416-3419.
21. Geisz, J.F., et al., *Enhanced external radiative efficiency for 20.8% efficient single-junction GaInP solar cells*. 2013. **103**(4).
22. global.sharp. Available from: <https://global.sharp/corporate/news/111104.html>.
23. Takamoto, T.J.J.o.A.P., *Thin film single and multi junction solar cells*. 1997. **36**: p. 6215-6220.
24. Jain, N., et al. *GaInAsP/GaInAs tandem solar cell with 32.6% one-sun efficiency*. in *2017 IEEE 44th Photovoltaic Specialist Conference (PVSC)*. 2017. IEEE.
25. Shahrjerdi, D., et al., *Ultralight high-efficiency flexible InGaP/(In) GaAs tandem solar cells on plastic*. 2013. **3**(5): p. 566-571.

-
26. Green, M.A., *Third generation photovoltaics*. 2006.
 27. Araki, K., et al. *Development of a robust and high efficiency concentrator receiver*. in *3rd World Conference on Photovoltaic Energy Conversion, 2003. Proceedings of*. 2003. IEEE.
 28. King, R., et al. *Pathways to 40%-efficient concentrator photovoltaics*. in *Proc. 20th European Photovoltaic Solar Energy Conference*. 2005.
 29. Lin, G.J., et al., *III-V multi-junction solar cells*, in *Optoelectronics-Advanced Materials and Devices*. 2013, IntechOpen London.
 30. Srinivas, B., et al., *Review on present and advance materials for solar cells*. 2015. **3**(2015): p. 178-182.
 31. Suhaimi, S., et al., *Materials for enhanced dye-sensitized solar cell performance: Electrochemical application*. 2015. **10**(4): p. 2859-2871.
 32. Bagher, A.M., et al., *Types of solar cells and application*. 2015. **3**(5): p. 94-113.
 33. Badawy, W.A.J.J.o.a.r., *A review on solar cells from Si-single crystals to porous materials and quantum dots*. 2015. **6**(2): p. 123-132.
 34. Dubey, S., J.N. Sarvaiya, and B.J.E.p. Seshadri, *Temperature dependent photovoltaic (PV) efficiency and its effect on PV production in the world—a review*. 2013. **33**: p. 311-321.
 35. Panigrahi, S., D.J.J.o.c. Basak, and i. science, *Morphology driven ultraviolet photosensitivity in ZnO–CdS composite*. 2011. **364**(1): p. 10-17.
 36. Park, N.-G.J.M.t., *Perovskite solar cells: an emerging photovoltaic technology*. 2015. **18**(2): p. 65-72.
 37. Shi, D., Y. Zeng, and W.J.S.r. Shen, *Perovskite/c-Si tandem solar cell with inverted nanopillars: realizing high efficiency by controllable light trapping*. 2015. **5**(1): p. 16504.
 38. Zhang, X., et al., *Effects of solvent coordination on perovskite crystallization*. 2021. **37**: p. 2008055.
 39. Hatem, D., F. Nemmar, and M.S.J.J.o.R.E. Belkaid, *Cellules solaires organiques: choix des matériaux, structures des dispositifs et amélioration du rendement et de la stabilité*. 2009. **12**(1): p. 77–86-77–86.
 40. Hadjab, M., *Développement des performances d'un système photovoltaïque*. 2011, Université El Djilali Liabès de Sidi Bel Abbès.
 41. Bendjelloul, Z.J.M.d.m.U.d.B., *Contribution à la modélisation d'une cellule solaire*. 2009.
 42. Petibon, S., *Nouvelles architectures distribuées de gestion et conversion de l'énergie pour les applications photovoltaïques*. 2009, Université Paul Sabatier-Toulouse III.
 43. Bayod-Rújula, A.A., *Solar photovoltaics (PV)*, in *Solar hydrogen production*. 2019, Elsevier. p. 237-295.
 44. Qazi, S., *Standalone photovoltaic (PV) systems for disaster relief and remote areas*. 2016: Elsevier.
 45. Pearsall, N., *Introduction to photovoltaic system performance*, in *The performance of photovoltaic (PV) systems*. 2017, Elsevier. p. 1-19.
 46. BOUTLILIS, F., *Modélisation et simulation des sources de production décentralisée Application à l'intégration d'un générateur PV à stockage dans un réseau électrique*. 2018, Thèse de Doctorat EN GENIE ELECTRIQUE, Université Abdelhamid Ibn Badis de
 47. Khatib, T., et al., *A review on sizing methodologies of photovoltaic array and storage battery in a standalone photovoltaic system*. 2016. **120**: p. 430-448.
 48. Fouad, M., et al., *An integrated review of factors influencing the performance of photovoltaic panels*. 2017. **80**: p. 1499-1511.
 49. Du, D., J. Darkwa, and G.J.S.E. Kokogiannakis, *Thermal management systems for photovoltaics (PV) installations: a critical review*. 2013. **97**: p. 238-254.
 50. Kaldellis, J.K., M. Kapsali, and K.A.J.R.e. Kavadias, *Temperature and wind speed impact on the efficiency of PV installations. Experience obtained from outdoor measurements in Greece*. 2014. **66**: p. 612-624.
-

51. Quaschnig, V. and R.J.S.e. Hanitsch, *Numerical simulation of current-voltage characteristics of photovoltaic systems with shaded solar cells*. 1996. **56**(6): p. 513-520.
52. Park, N., W. Oh, and D.J.I.J.o.P. Kim, *Effect of temperature and humidity on the degradation rate of multicrystalline silicon photovoltaic module*. 2013. **2013**(1): p. 925280.
53. Panjwani, M.K., G.B.J.I.J.o.E.R. Narejo, and G. Science, *Effect of humidity on the efficiency of solar cell (photovoltaic)*. 2014. **2**(4): p. 499-503.
54. Sahay, A., et al., *A review of solar photovoltaic panel cooling systems with special reference to Ground coupled central panel cooling system (GC-CPCS)*. 2015. **42**: p. 306-312.
55. Elminshawy, N.A., et al., *The performance of a buried heat exchanger system for PV panel cooling under elevated air temperatures*. 2019. **82**: p. 7-15.
56. Elminshawy, N.A., et al., *Performance of PV panel coupled with geothermal air cooling system subjected to hot climatic*. 2019. **148**: p. 1-9.
57. Lopez-Pascual, D., et al., *Experimental characterization of a geothermal cooling system for enhancement of the efficiency of solar photovoltaic panels*. 2022. **8**: p. 756-763.
58. Kadhim, A.M. and I.M.A.J.H.T. Aljubury, *Experimental performance of cooling photovoltaic panels using geothermal energy in an arid climate*. 2021. **50**(3): p. 2725-2742.
59. Yang, L.-H., et al., *Enhanced efficiency of photovoltaic panels by integrating a spray cooling system with shallow geothermal energy heat exchanger*. 2019. **134**: p. 970-981.
60. Jafari, R.J.S.E., *Optimization and energy analysis of a novel geothermal heat exchanger for photovoltaic panel cooling*. 2021. **226**: p. 122-133.
61. Ruoping, Y., et al., *Study of operation performance for a solar photovoltaic system assisted cooling by ground heat exchangers in arid climate, China*. 2020. **155**: p. 102-110.
62. Babasaci, A., I. Bouguenara, and A. Chaouche, *Etude de la performance d'un échangeur de chaleur air-sol couplé avec la cheminée solaire pour des applications de chauffage et de refroidissement dans les régions arides*.
63. DIDA, M., *Etude et amélioration des systèmes de conversion photovoltaïque dans les zones arides et semi-arides*. 2022.
64. ONM. *National Office of Meteorology. Climate data of Ouargla*. Available from: <https://www.meteo.dz/>.
65. maps, A.; Available from: <https://nelson.wisc.edu/sage> data-and-models/atlas/maps/avganntemp/atl_avganntemp_afr.jpg, (Accessed 29/07/2020).

ملخص

نقدم في هذا العمل دراسة تجريبية لتحسين كفاءة الألواح الكهروضوئية من خلال استخدام نظام التبريد بالطاقة الحرارية الأرضية، تم في هذه دراسة تجريبية ربط نظام التبريد بالطاقة الحرارية الأرضية بالجزء الخفي للوح كهروضوئي بواسطة غطاء من الألومنيوم يسمح بصنع فجوة لمرور تيار الهوائي المتدفق من الانبوب المدفون تحت الأرض. حيث أظهرت النتائج المحصل عليها على ان درجة حرارة اللوح المبرد انخفضت بنسبة 6 درجات مئوية عن درجة حرارة اللوح الغير مبرد. ووجدنا أيضا انه كلما كانت سرعة تدفق الهواء عالية كان تبريد اللوح الكهروضوئي أسرع. يمكن ان نعتبر ان نظام التبريد بالطاقة الحرارية الأرضية يعتبر حلا من الطول لمشكل ارتفاع درجة حرارة الخلايا الكهروضوئية.

الكلمات المفتاحية: الخلايا الكهروضوئية؛ التبريد الكهروضوئي؛ درجة الحرارة؛ الطاقة الحرارية الأرضية.

summary

In this work, we present an experimental study to improve the efficiency of photovoltaic panels through the use of a geothermal cooling system. In this pilot study, the geothermal cooling system was attached to the back of the PV panel using an aluminum cover that allowed a gap for a irflow flowing from the underground pipe. The results obtained showed that the temperature of the cooled panel decreased by 6°C compared to the temperature of the non-cooled panel. We also found that the faster the airflow, the faster the PV panel cools. We can consider geothermal cooling system as one of the solutions to the problem of photovoltaic cell overheating.

Keywords: photovoltaic cells; Photoelectric cooling. Temperature; Geothermal energy.